A MANUAL

FOR

AMPS-1D

ParsOptics Group

A ONE-DIMENSIONAL DEVICE SIMULATION PROGRAM FOR THE ANALYSIS OF MICROELECTRONIC AND PHOTONIC STRUCTURES

AMPS-1D was developed with the support of the Electric Power Research Institute and equipment support by IBM. AMPS-1D is the creation of Professor Stephen J. Fonash and the following Students and Post-Docs:

J. Arch, J. Hou, W. Howland, P. McElheny, A. Moquin, M. Rogosky, F. Rubinelli , T. Tran and H. Zhu.

The Electronic Materials and Processing Research Laboratory
The Pennsylvania State University
University Park, PA 16802

CONTENTS

PREFACE

AMPS is a very general program for analyzing and designing transport in microelectronic and photonic structures. It differs from other transport analysis programs such as PICES in a number of ways. Among them are its ability to handle any defect and doping energy gap and special distribution, its incorporation of S-R-H and band-to-band recombination, its incorporation of Boltzmann and Fermi-Dirac statistics, its ability to handle varying material properties, its very general treatment of contacts, and its ability to handle transport in devices under voltage bias, light bias, or both.

This manual for AMPS-1D is intended for those using our window '95/NT version. We apologize in advance for the fact that this manual will get out of date but, as we are sure you understand, AMPS is a constantly growing, developing package. However, most of what is said here will remain valid and should be useful.

AMPS would not exist without the support of the Electric Power Research Institute. In particular it would not exist without the encouragement, guidance, and questioning of Dr. Terry Peterson of EPRI and without the vision of Dr. Ed DeMeo and Dr. John Crowley.

Stephen Fonash
Electronic Materials and Processing Research Laboratory
Penn State University

FIGURES

CHAPTER 1
INTRODUCTION

1.1 AMPS and Its Features

This manual is an introduction to a very general, one-dimensional computer program for simulating transport physics in solid state devices. It uses the first-principles continuity and Poisson's equations approach to analyze the transport behavior of semiconductor electronic and opto-electronic device structures. These device structures can be composed of crystalline, polycrystalline, or amorphous materials or combinations thereof. This program, called AMPS (**A**nalysis of **M**icroelectronic and **P**hotonic **S**tructures), numerically solves the three governing semiconductor device equations (the Poisson equation and the electron and hole continuity equations) without making any a-priori assumptions about the mechanisms controlling transport in these devices. With this general and exact numerical treatment, AMPS may be used to examine a variety of device structures that include

- homojunction and heterojunction p-n and p-i-n, solar cells and detectors;
- homojunction and heterojunction p-n, p-i-n, n-i-n, and p-i-p microelectronic structures;
- multi-junction solar cell structures;
- multi-junction microelectronic structures;
- compositionally-graded detector and solar cell structures;
- compositionally-graded microelectronic structures;
- novel device microelectronic, photovoltaic, and opto-electronic structures;
- Schottky barrier devices with optional back layers.

From the solution provided by an AMPS simulation, output such as current voltage characteristics in the dark and, if desired, under illumination can be obtained. These may be computed as a function of temperature. For solar cell and detector structures, collection efficiencies as a function of voltage, light bias, and temperature can also be obtained. In addition, important information such as electric field distributions, free and trapped carrier populations, recombination profiles, and individual carrier current densities as a function of position can be extracted from the AMPS program. As stated earlier, AMPS' versatility can be used to analyze transport in a wide variety of device structures that can contain combinations of crystalline, polycrystalline, or amorphous layers. AMPS is formulated to analyze, design, and optimize structures intended for microelectronic, photovoltaic, or opto-electronic applications.

A comparison of AMPS with other known programs shows that AMPS is the only computer modeling program available that incorporates all of the following physics:

- a contact treatment that allows thermionic emission and recombination to take place at device contacts;

- a very generalized gap state model that can fit any density of states distribution in the bulk or at an interface;
- both band-to-band and Shockley-Read-Hall recombination;
- a recombination model that computes Shockley-Read-Hall recombination traffic through any inputted general gap state distribution instead of the often-used single recombination level approach;
- full Fermi-Dirac, and not just Boltzmann, statistics;
- gap state populations computed with actual-temperature statistics rather than the often used T=0K approach;
- a trapped charge model that accounts for charge in any inputted general gap state distribution;
- a gap state model that allows capture cross-sections to vary with energy;
- gap state distributions whose properties can vary with position;
- carrier mobility that can vary with position;
- electron and hole affinities that can vary with position;
- mobility gaps that can differ from optical gaps;
- the ability to calculate device characteristics as a function of temperature in both forward and reverse bias as well as with or without illumination;
- the ability to analyze device structures fabricated using single crystal, polycrystalline, or amorphous materials or all three.

1.2 About This Manual

This manual assumes the user has completed an introductory course in semiconductor device physics and is familiar with mathematical concepts such as Poisson's equation and the continuity equations. A working knowledge of numerical methods is helpful, but not actually required for working with the AMPS program. This manual explains the approach used in AMPS for

- modeling of hole and electron transport, including a discussion of the basic equations and solution techniques (Chapter 2);
- parameterizing material properties (Chapter 3)
  - semiconductor materials
  - insulators
  - metals
  - interfaces
  - materials with position dependent properties;

- running programs to obtain band diagrams in thermodynamic equilibrium and for running programs for devices under voltage, light bias, or both (non-thermodynamic equilibrium) (Chapter 5).

The manual begins by using the introductory chapter to offer a brief overview of AMPS, and to present some examples of its capabilities. Chapter 2 can be skipped but it has been included in this manual for those who are interested it discusses the physical and mathematical bases of the simulation programs. Chapter 3 discusses parameterizing material properties and it shows that close attention must be given to the particular types of materials the user intends to "build" his or her structure. The AMPS programs will ask the user to input these specific parameters. Chapter 4 describes the heart of AMPS: the procedures for obtaining the detailed physics and terminal characteristics of devices under voltage bias, light bias, or both.

1.3 An Overview of How AMPS Works

In briefly overviewing our methods of modeling microelectronic and opto-electronic devices, we first note that the physics of device transport can be captured in three governing equations: Poisson's equation, the continuity equation for free holes, and the continuity equation for free electrons. Determining transport characteristics then becomes a task of solving these three coupled non-linear differential equations, each of which has two associated boundary conditions. In AMPS, these three coupled equations, along with the appropriate boundary conditions, are solved simultaneously to obtain a set of three unknown state variables at each point in the device: the electrostatic potential, the hole quasi-Fermi level, and the electron quasi-Fermi level. From these three state variables, the carrier concentrations, fields, currents, etc. can then be computed. To determine these state variables, the method of finite differences and the Newton-Raphson technique are incorporated by the computer. The Newton-Raphson Method iteratively finds the root of a function or roots of a set of functions if given an adequate initial guess for these roots. In AMPS, the one-dimensional device being analyzed is divided into segments by a mesh of grid points, the number of which the user decides. The three sets of unknowns are then solved for each particular grid point. We note that AMPS allows the mesh to have variable grid spacing at the discretion of the user. As noted, once these three state variables are obtained as a function of x, the band edges, electric field, trapped charge, carrier populations, current densities, recombination profiles, and any other transport information may be obtained.

1.4 Examples of AMPS Output

The following examples illustrate the different types of semiconductor structures that AMPS can simulate and also give a sampling of the output information AMPS can generate. These are just two straight-forward examples intended to give the reader some indication of the power and versatility of AMPS.

1.4.1 An example — a $Al_{0.3}Ga_{0.7}As$/GaAs Heterojunction Diode

Figures 1-1. and 1-2. give the room-temperature current-voltage characteristic in forward and reverse bias and the band structure in thermodynamic equilibrium for an $Al_{0.3}Ga_{0.7}As$/GaAs p-n heterojunction diode. The doping happens to have been taken to be 10^{16} cm^{-3} in both layers.

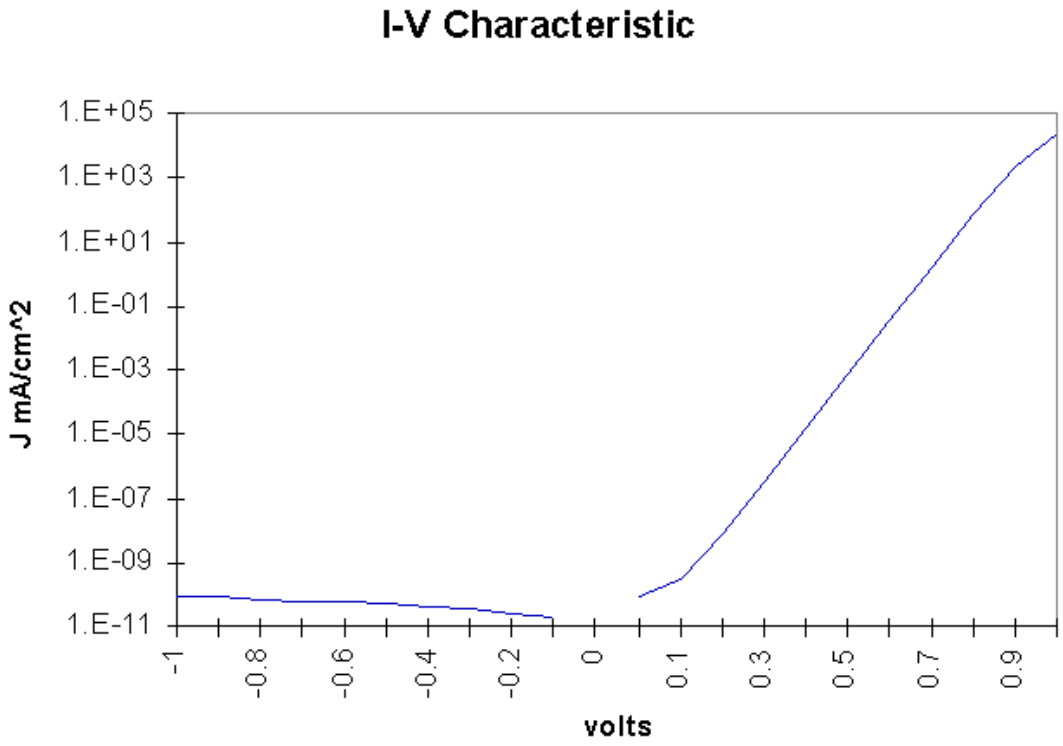

Figure1-1 Current-Voltage characteristic in forward and reverse bias.

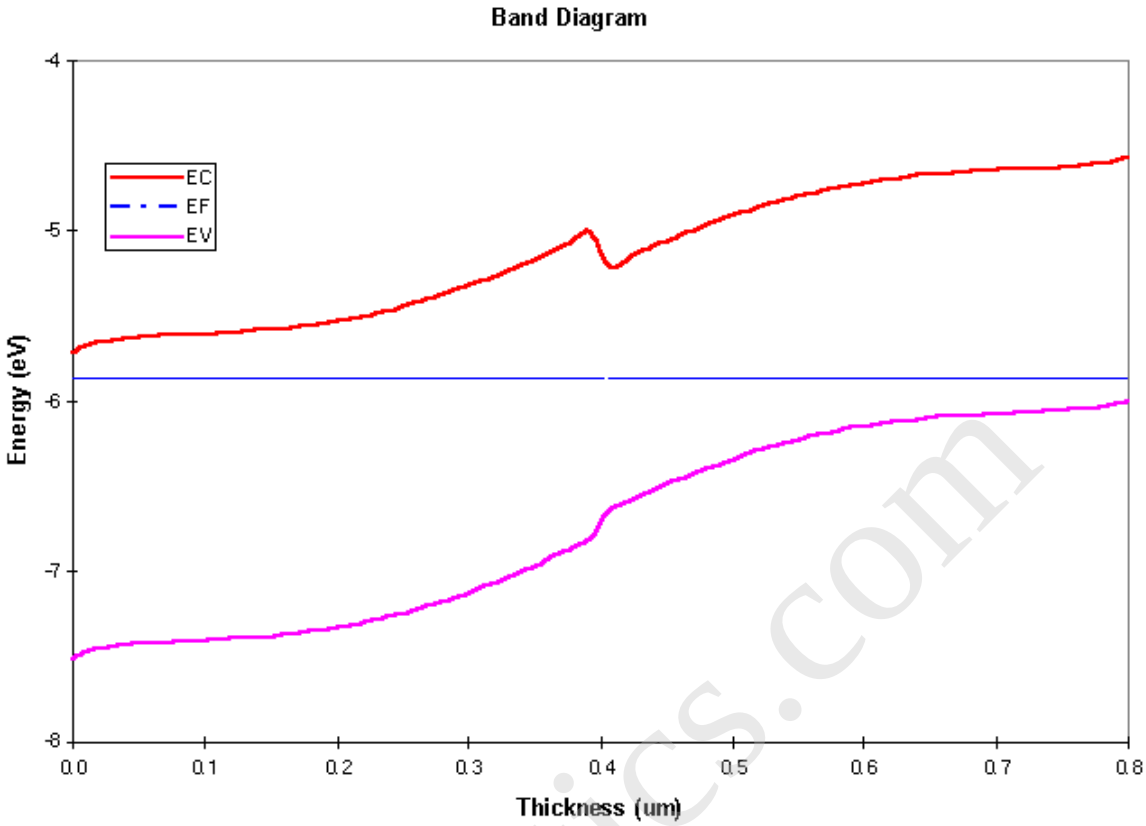

Figure1-2 Band structure in thermodynamic equilibrium.

Figure 1-3. shows the space charge at -1, 0, and +1 volts (i.e., forward, zero, and reverse biases, respectively). This example demonstrates how AMPS can be used to determine the amount of charge transfer in the space charge regions of heterojunction structures and the widths of these space charge layers as a function of bias. The current-voltage characteristic, along with other output from AMPS, can be used to determine how different transport mechanisms become important at different magnitudes of forward and reverse bias.

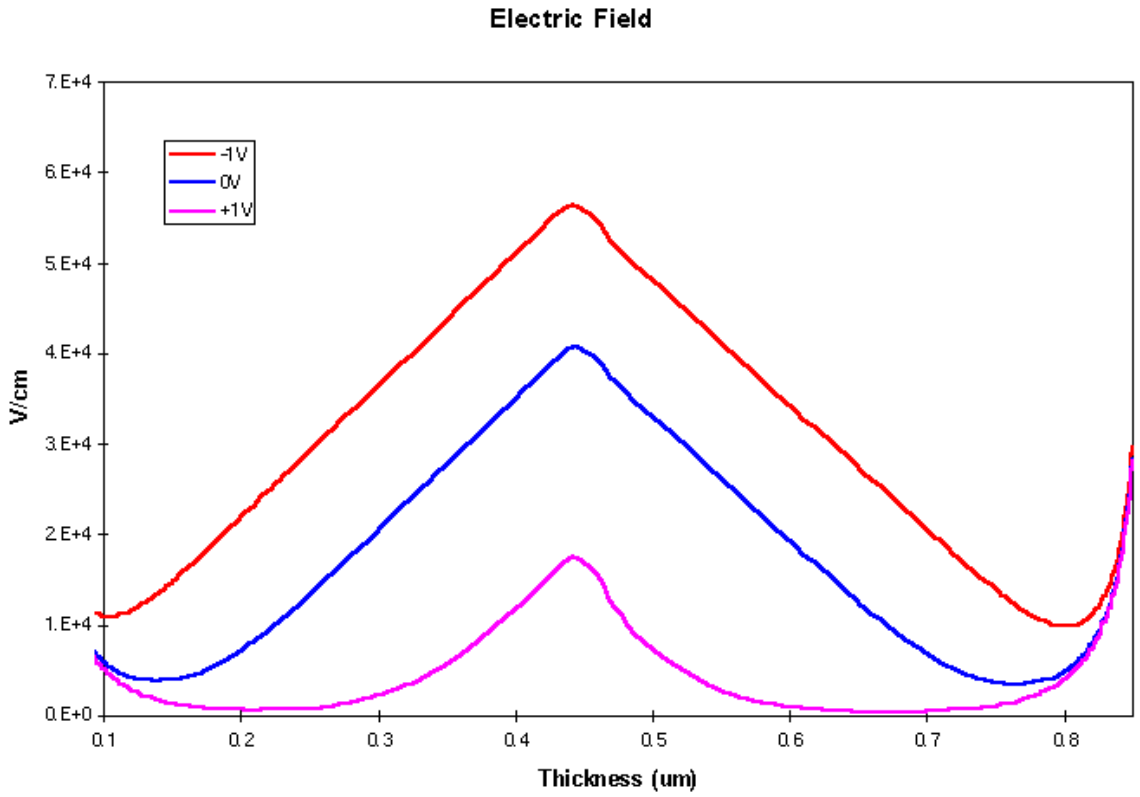

Figure 1-3 Spatial dependence of the electric field at three different bias voltages. -1V, 0V, 1V.

1.4.2 An Example — a Triple Junction Solar Cell

Figure 1-4. gives the illuminated current-voltage characteristic and the cell performance values obtained from AMPS simulation of an a triple p-i-n solar cell. The density of states used to model the a-Si:H materials consists of exponential tail states and midgap states. Fig 1-5. shows the band diagram of this complicated cell in thermodynamic equilibrium. Figure 1-6 shows the electron and hole lifetime at open circuit voltage. This example illustrates AMPS usefulness in determining the transport mechanisms controlling cell performance and in optimizing cell design. In addition, this final example also highlights the versatility of AMPS by demonstrating its ability to model complicated structures with many layers of different materials.

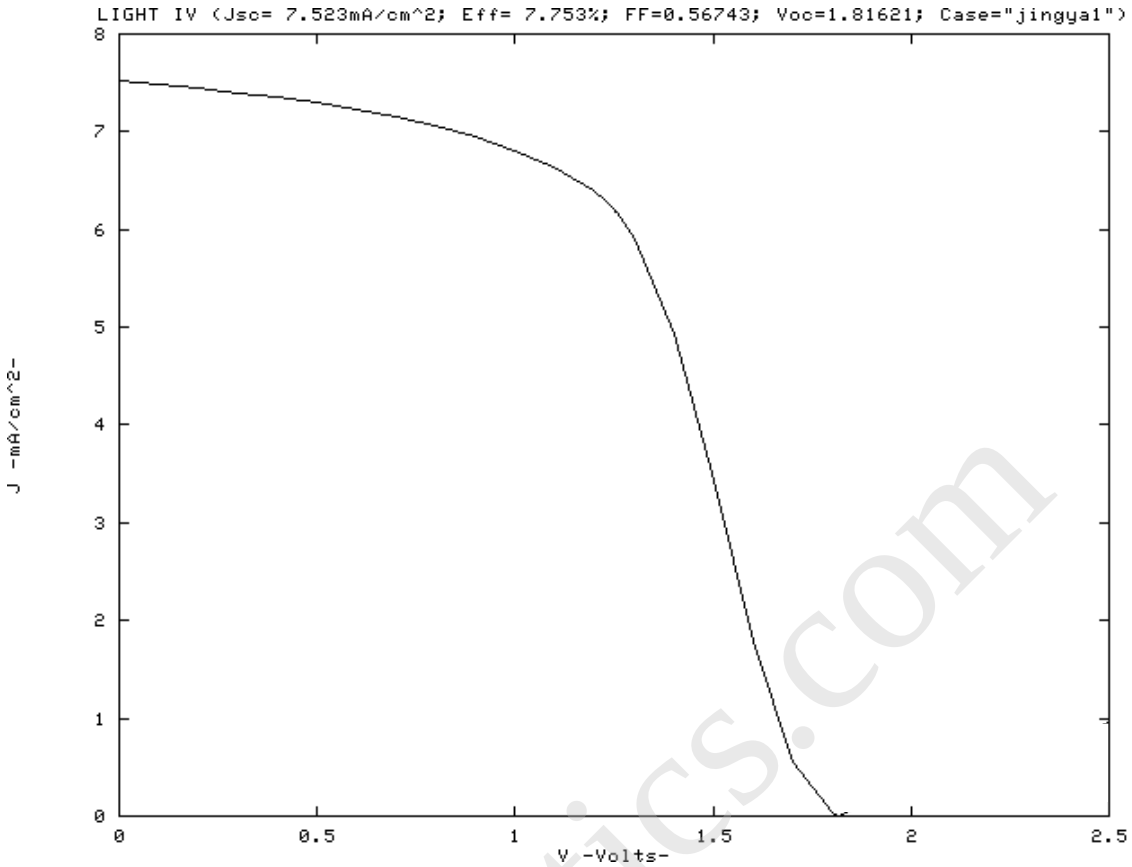

Figure 1-4. Illuminated current-voltage characteristic and cell performance values for this triple junction solar cell.

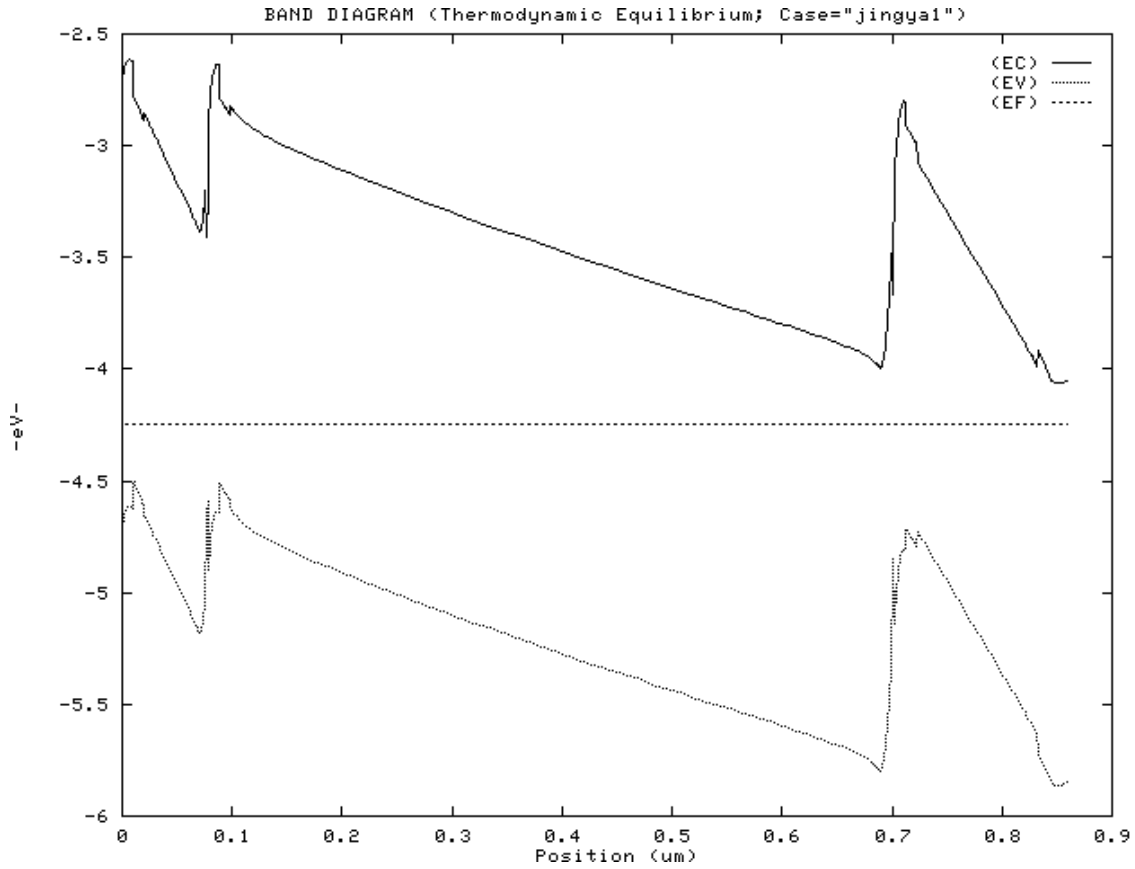

Figure 1-5. Band diagram of this triple junction in thermodynamic equilibrium.

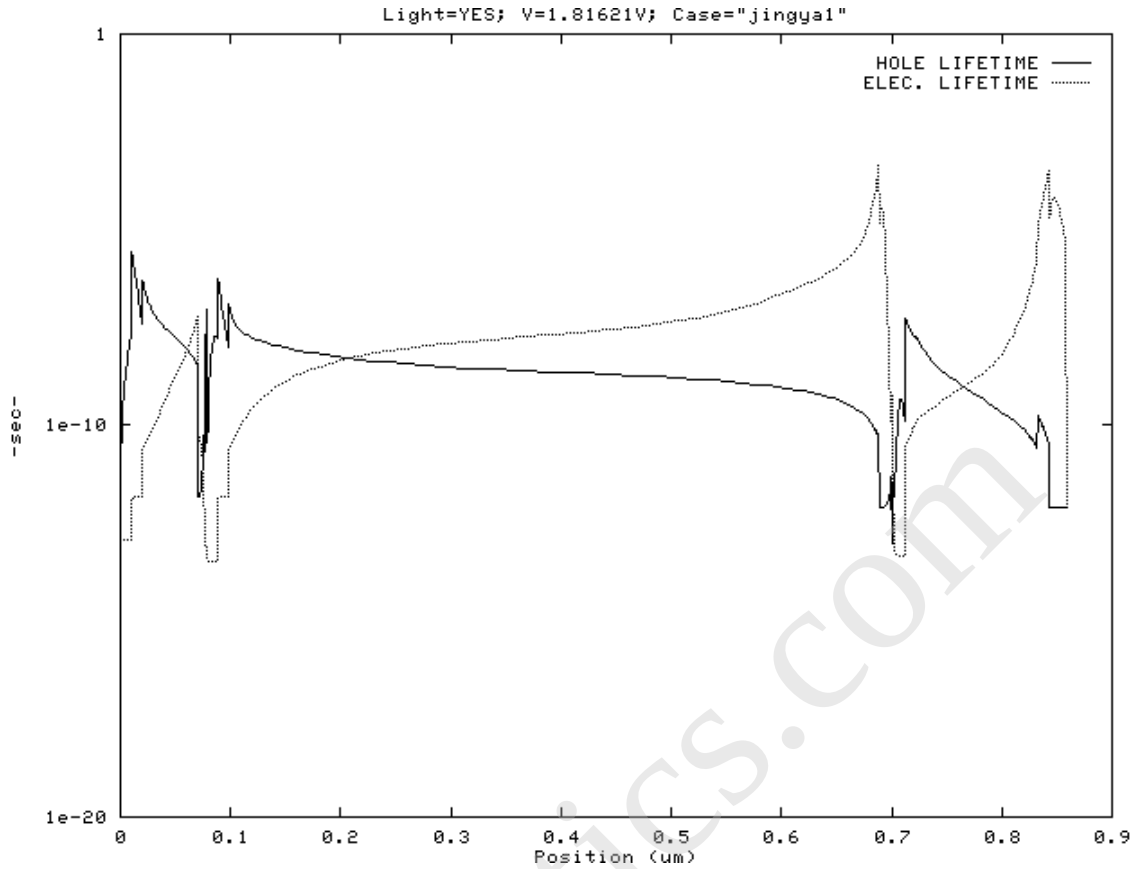

Figure 1-6. Electron and hole lifetime at V_{OC} versus position for a triple. Only meaningful for regions where carrier is the minority carrier.

CHAPTER 2
MATHEMATICAL MODELING & SOLUTION TECHNIQUES

2.0 Introduction

As noted in Chapter 1, this chapter may be skipped. It is intended for those who want to "open AMPS up and get an idea how it ticks."

Understanding of how AMPS "ticks" begins by noting that with the continuum approach used in AMPS, the physics of device transport can be captured in three governing equations: Poisson's equation, the continuity equation for free holes, and the continuity equation for free electrons. Determining transport characteristics then becomes a task of solving these three coupled non-linear differential equations subject to appropriate boundary conditions. These three equations and the corresponding boundary conditions, along with the numerical solution technique used to solve them, will then be the subject of this chapter.

We assume in AMPS that the material system under examination is in steady state. That is, it is assumed that there is no time dependence. It follows that the terminal characteristics generated by AMPS are the quasi-static characteristics.

2.1 Poisson's Equation

Poisson's equation links free carrier populations, trapped charge populations, and ionized dopant populations to the electrostatic field present in a material system. In one-dimensional space, Poisson's equation is given by

$$\frac{d}{dx}\left(-\varepsilon(x)\frac{d\Psi'}{dx}\right) = q\cdot\left[p(x)-n(x)+N_D^{+}(x)-N_A^{-}(x)+p_t(x)-n_t(x)\right]$$

where the electrostatic potential Ψ' and the free electron n, free hole p, trapped electron n_t, and trapped hole p_t, as well as the ionized donor-like doping N_D^+ and ionized acceptor-like doping N_A^- concentrations are all functions of the position coordinate x. Here, ε is the permittivity and q is the magnitude of the charge of an electron.

Since band diagrams show the energies allowed to electrons and since the electrostatic potential Ψ' is defined for a unit positive particle, the use of Ψ' in the above equation can be inconvenient. The local vacuum level E_{VL}, which is the top or escape energy of the conduction band, varies only due to the presence of an electrostatic field [1]. Its derivative, therefore, is proportional to the electrostatic field ξ. In fact, if we remember to measure the position of the local vacuum level from a reference using the quantity Ψ measured in eV, then $\xi = d\Psi/dx$. As seen in Fig. 2-1, AMPS uses Ψ not Ψ' and always chooses the reference for Ψ to be the position of the local vacuum level in the contact at the right hand side of any general device structure. With this particular example in Fig. 2-1 of a Schottky barrier Ψ, as we have defined it, is seen to be a negative quantity in much of the

n^+ back-contact layer and a positive quantity essentially through the remainder of the device. Using this way of locating the local vacuum level and remembering that its spatial derivative is the electrostatic field allows us to rewrite Poisson's equation in terms of the local vacuum level Ψ measured in eV. This gives

$$\frac{d}{dx}\left(\varepsilon(x)\frac{d\Psi}{dx}\right) = q\cdot\left[p(x)-n(x)+N_D^+(x)-N_A^-(x)+p_t(x)-n_t(x)\right] \qquad (2.1)$$

Equation (2.1) is the form of Poisson's equation that AMPS uses.

Having settled on a formulation of Poisson's equation that will be convenient, we now realize that AMPS needs expressions for the six new dependent variables n, p, n_t, p_t, N_D^+, and N_A^- introduced in Equation 2.1.

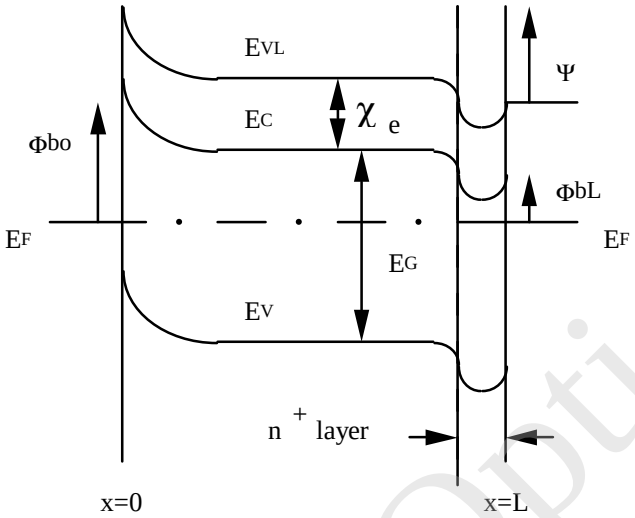

Figure 2-1. A band diagram of a Schottky barrier in thermodynamic equilibrium.

2.1.1 The Delocalized (Band) State Populations n and p

Assuming that a parabolic relation between the density of states N(E) of the delocalized states of the bands and the energy E - measured positively moving away from either band edge - exists such that $N(E) \propto E^{1/2}$, the free carrier concentrations in thermodynamic equilibrium or under voltage bias, light bias, or both are computed in AMPS using the general expressions [2]

$$n = N_c F_{1/2} \exp\left(\frac{E_F-E_c}{kT}\right) \qquad (2.1.1a)$$

$$p = N_v F_{1/2} \exp\left(\frac{E_V-E_F}{kT}\right) \qquad (2.1.1b)$$

These general expressions allow for the possibility of degeneracy; i.e. AMPS includes both Fermi-Dirac and Boltzmann statistics. In these expressions N_c and N_v are the band effective densities of states for the conduction and valence bands, respectively. In AMPS these are user chosen material parameters. For crystalline materials they are given by [2]

$$N_C = 2\left(\frac{2\pi m_n^* kT}{h^2}\right)^{3/2} \tag{2.1.1c}$$

$$N_V = 2\left(\frac{2\pi m_p^* kT}{h^2}\right)^{3/2} \tag{2.1.1d}$$

where m_n^* is the electron effective mass, m_p^* is the hole effective mass, k is the Boltzmann constant, and h is Planck's constant.

The Fermi integral of order one-half appearing in Equation 2.1.1a and b is defined as [6]

$$F_{1/2}(\eta) = \frac{2}{\sqrt{\pi}} \int_0^\infty \frac{E^{1/2}\, dE}{1 + \exp(E - \eta)} \tag{2.1.1e}$$

$E^{1/2}$ where η - the Fermi integral argument - is expressed as

$$\eta_n = \left(\frac{E_F - E_C}{kT}\right) \tag{2.1.1f}$$

for free electrons and

$$\eta_p = \left(\frac{E_V - E_F}{kT}\right) \tag{2.1.1g}$$

for free holes. We note that for $\eta_n > 3$ or $\eta_p > 3$, the function $F_{1/2}$ reduces to the corresponding Boltzmann factors

$$\exp\left(\frac{E_F - E_c}{kT}\right) \tag{2.1.1h}$$

or

$$\exp\left(\frac{E_v - E_F}{kT}\right) \tag{2.1.1i}$$

In our formulation of AMPS we have chosen to write n and p in terms of Boltzmann factors yet to allow the possibility of degeneracy and the need for Fermi-Dirac statistics. To do this we define the Fermi-Dirac degeneracy factor γ as

$$\gamma_n = \frac{F_{1/2}(\eta_n)}{\exp(\eta_n)} \tag{2.1.1j}$$

for free electrons and as

$$\gamma_p = \frac{F_{1/2}(\eta_p)}{\exp(\eta_p)} \tag{2.1.1k}$$

for free holes. With these definitions Equations 2.1.1a and 2.1.1b become

$$n = N_C \gamma_n \exp(\eta_n) \tag{2.1.1l}$$

$$p = N_V \gamma_n \exp(\eta_p) \qquad (2.1.1m)$$

which are valid for degenerate as well as non-degenerate situations.

When a device is driven out of thermodynamic equilibrium by a voltage bias, a light bias, or both the quantities n and p can still be computed using Equations 2.1.1a - 2.1.1e. It is only necessary to replace the equilibrium Fermi-level E_F with the quasi-Fermi level E_{Fn} in Equation 2.1.1a and the quasi-Fermi level E_{Fp} in Equation 2.1.1b. This is what AMPS does in going from thermodynamic equilibrium to cases with voltage bias, light bias, or both.

2.1.2 Localized (Gap) State Populations N_D^+, N_A^-, n_t, and p_t

Having obtained expressions for the n and p terms appearing in Poisson's equation, we must now develop expressions for the other quantities contributing to the development of charge. Since we have accounted for all the free charge, any additional charge must be in gap states.

In general there may be a variety of different types of gap (i.e., localized) states existing in the energy gap of a semiconductor or insulator. AMPS breaks these into states that are inadvertently present due to defects and impurities and into states that are purposefully present due to doping. There may be donor-like and acceptor-like states among both classes. There may also be states that are continuously distributed in energy or discretely distributed in energy in both classes. AMPS allows for different distributions of these states at interfaces and at different places in the bulk material.

In the case of the gap states which are not purposefully present, but are due to defects and impurities, AMPS defines n_t as being the number of charged acceptor-like sites per volume (i.e., trapped electrons) and p_t as being the number of charged donor-like sites per volume (i.e., trapped holes) in this class of states. In the case of the gap states which are purposefully present due to doping AMPS defines N_A^- as being the number of ionized acceptor-dopant sites per volume. Correspondingly N_D^+ is defined as being the number of ionized donor-dopant sites per volume.

2.1.2.1 Doping Levels (N_D^+ and N_A^-)

We turn first to the charge residing in localized doping levels. The doping levels in our usage include gap states which are characterized by discrete levels and gap states that form a band with a bandwidth defined by an upper energy boundary and a lower energy boundary. This latter case of localized gap state bands can arise if heavy doping is present in a structure. It is important to note that any combination of these two unique types of states is acceptable to AMPS (see section 2.1.2.1c). In any case, the total charge arising in these states can be represented by

$$N_D^+ = N_{dD}^+ + N_{bD}^+ \qquad (2.1.2.1a)$$

for the donor-dopant levels and

$$N_A^- = N_{dA}^- + N_{bA}^- \qquad (2.1.2.1b)$$

for the acceptor-dopant levels. Here, N_D^+ and N_A^- seen in Poisson's equation (Equation 2.1), are the total charges arising from both the discrete and banded dopant energy levels. In these equations

N_{dD}^{+} and N_{dA}^{-} represent the total charge originating from discrete donor and acceptor concentrations, respectively, while N_{bD}^{+} and N_{bA}^{-} represent the total charge developed by any banded donor and acceptor levels, respectively.

2.1.2.1a Discrete Dopant Levels ($N_{dD,i}$and $N_{dA,j}$)

Discrete localized dopant sites are located at single energy levels and arise from the intentional introduction of impurities. These states are illustrated pictorially by Figure 2-2.

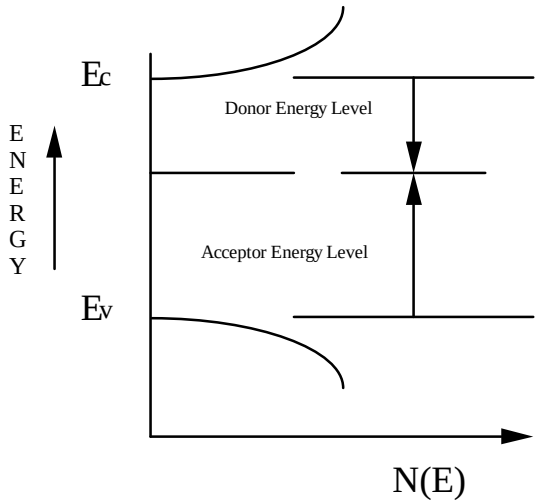

Figure 2-2. Density of states plot representing discrete localized dopant levels. The donor levels are located positively down from the conduction band and the acceptor levels are located positively up from the valence band.

The charge arising from a set of i of these discrete dopant states can be expressed as

$$N_{dD}^{+} = \sum_{i} N_{dD,i}\,\mathbf{f}_{D,i} \qquad (2.1.2.1c)$$

if they are donor-like and from a set of j of these discrete dopant states as

$$N_{dA}^{-} = \sum_{i} N_{dA,j}\,\mathbf{f}_{A,j} \qquad (2.1.2.1d)$$

if they are acceptor-like. Here N_{dD}^{+} and N_{dA}^{-},represent the discrete donor and acceptor charge, respectively. We allow for a number of these levels in AMPS with volume concentrations of $N_{dD,i}$ and $N_{dA,j}$ corresponding to the donor level energy E_i and the acceptor level energy E_j, respectively. The number of these doping sites per volume and their energy levels may even vary with position in AMPS as specified by the user. The quantity $\mathbf{f}_{D,i}$ is the probability that a discrete-level donor site of energy E_i has lost an electron and $\mathbf{f}_{A,j}$ is the probability that a discrete level acceptor site of energy E_j has gained an electron. In thermodynamic equilibrium, the occupation probabilities $\mathbf{f}_{D,i}$ and $\mathbf{f}_{A,j}$ are represented by one minus the Fermi function and by the Fermi function, respectively. That is, in thermodynamic equilibrium

$$\mathbf{f}_{D,i} = \frac{1}{1+\exp\left(\frac{E_F - E_i}{kT}\right)} \qquad (2.1.2.1e)$$

and

$$\mathbf{f}_{A,j} = \frac{1}{1+\exp\left(\frac{E_j - E_F}{kT}\right)} \qquad (2.1.2.1f)$$

Under bias, however, the above two expressions must be modified. The occupation probabilities now must be determined by the kinetics of electron capture and emission and hole capture and emission for the doping level in question. Using the Shockley-Read-Hall (S-R-H) model for these processes, and assuming that a donor-like discrete gap state of energy E_i in the gap communicates with the conduction band and the valence band only, allows us to write [1]

$$\mathbf{f}_{D,i} = \frac{\sigma_{pdD_i} \cdot p + \sigma_{ndD_i} \cdot \gamma_{n_i} \cdot n1_i}{\sigma_{ndD_i}(n+\gamma_{n_i} \cdot n1_i) + \sigma_{pdD_i}(p+\gamma_{p_i} \cdot p1_i)} \qquad (2.1.2.1g)$$

The corresponding expression for the jth discrete acceptor-like gap state of energy E_j in the gap is

$$\mathbf{f}_{A,j} = \frac{\sigma_{ndA_j} \cdot n + \sigma_{pdA_j} \cdot \gamma_{p_j} \cdot p1_j}{\sigma_{ndA_j}(n+\gamma_{n_j} \cdot n1_j) + \sigma_{ndA_j}(p+\gamma_{p_j} \cdot p1_j)} \qquad (2.1.2.1h)$$

In these expressions $\sigma_{ndD_i}(E_i)$ and $\sigma_{pdD_i}(E_i)$ are the capture cross sections for electrons and holes of the ith donor-like discrete levels, respectively. $\sigma_{ndA_j}(E_j)$ and $\sigma_{pdA_j}(E_j)$ are the capture cross section for electrons and holes at the jth acceptor site, and $n_{1_k}(E_k)$ and $p_{1_k}(E_k)$ are parameters that can be expressed as

$$n_{1_k}(E_k) = N_c \exp\left(\frac{E_k - E_c}{kT}\right) \qquad (2.1.2.1i)$$

$$p_{1_k}(E_k) = N_v \exp\left(\frac{E_v - E_k}{kT}\right) \qquad (2.1.2.1j)$$

In Equation 2.1.2.1g the degeneracy factor γ_{n_i} is given by

$$\gamma_{n_i} = \frac{F_{1/2}(\eta_{n_i})}{\exp(\eta_{n_i})} \qquad (2.1.2.1k)$$

where the argument η_{n_i} is expressed as

$$\eta_{n_i} = \left(\frac{E_F - E_i}{kT}\right) \qquad (2.1.2.1l)$$

Likewise, in Equation 2.1.2.1h the degeneracy factor for holes in the valence band is

$$\gamma_{n_j} = \frac{F_{1/2}(\eta_{n_j})}{\exp(\eta_{n_j})} \qquad (2.1.2.1m)$$

where the argument η_{p_j} is expressed as

$$\eta_{n_i} = \left(\frac{E_i - E_F}{kT} \right) \qquad (2.1.2.1n)$$

We point out that our formulation for N_{dD}^{+} and N_{dA}^{-} allows for degeneracy and allows for both S-R-H and band-to-band recombination to be present. We note that Equations 2.1.2.1g and h can be used in the form shown which involves the free carrier populations or they can be recast into an alternative form which would be like Equations 2.1.2.1e and f with appropriately defined gap state quasi-Fermi levels. Unfortunately the latter course of action necessitates, in general, defining a gap state quasi-Fermi level for each discrete donor and acceptor level. In AMPS we avoid the use of quasi-Fermi levels for each set of gap states and use Equations 2.1.2.1g and h for $\mathbf{f}_{D,i}$ and $\mathbf{f}_{A,j}$ for systems under bias and Equations 2.1.2.1e and f for $\mathbf{f}_{D,i}$ and $\mathbf{f}_{A,j}$ for systems in thermodynamic equilibrium.

2.1.2.1b Banded Dopant Levels ($N_{bD,i}$ and $N_{bA,j}$)

Banded localized dopant sites are located within an energy band which has a lower boundary E_1 and an upper boundary E_2. These energies are measured positively down from E_C for donor states and positively up from E_V for acceptor states. They are shown in Figure 2-3..

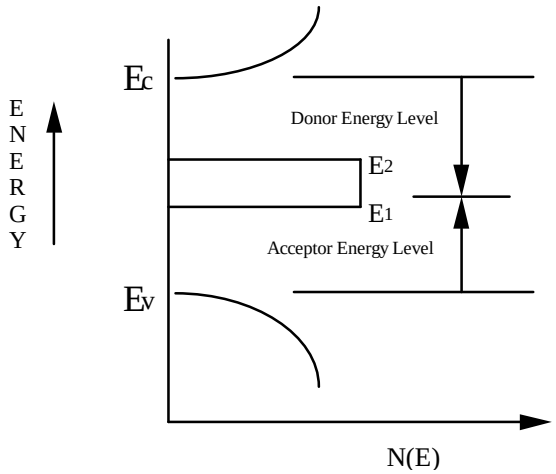

Figure 2-3. Density of states plot showing a band of dopant states. Energies for donor sites are measured positively down to E_1 from the conduction band and those for acceptor sites are measured positively up to E_1 from the valence band.

The charge arising from dopant states can be expressed as

$$N_{bD}^{+} = \sum_i N_{bD,i}^{+} \qquad (2.1.2.1o)$$

if they are donor-like states and as

$$N_{bA}^{-} = \sum_i N_{bA,j}^{-} \qquad (2.1.2.1p)$$

if they are acceptor-like states. Here N_{bD}^{+} and N_{bA}^{-}, are the charges arising from the banded donor and acceptor energy levels. We allow for a number of these banded levels with band i of donor-like

states having a site concentration of $N_{bD,i}^{+}$ and band j of acceptor-like banded states having a site concentration of $N_{bA,j}^{-}$.

Considering the i^{th} band of banded dopant donor states we assume the concentration across the width of the band, defined by $W_{Di} = E_{2i}-E_{1i}$, to be $N_{bD,i}$ states per volume. Hence, $N_{bD,i}^{+}$ coming from these states is

$$N_{bD,i}^{+} = \frac{N_{D_i}}{W_{D_i}} \int_{E_{1_i}}^{E_{2_i}} f_{D_i}(E)\, dE, \qquad W_{D_i} = E_{2_i}-E_{1_i} > 0 \tag{2.1.2.1q}$$

Corresponding to the j^{th} band of banded acceptor dopant levels, we obtain

$$N_{bA,j}^{-} = \frac{N_{A_j}}{W_{A_j}} \int_{E_{1_j}}^{E_{2_j}} f_{A_j}(E)\, dE, \qquad W_{A_j} = E_{2_j}-E_{1_j} > 0 \tag{2.1.2.1r}$$

The quantity f_{bD_i} is the probability that one of these dopant donor sites of energy between E and E+dE has lost an electron and f_{bA_j} is the probability that one of these dopant acceptor sites of energy between E and E+dE has gained an electron. In thermodynamic equilibrium, the occupation probabilities f_{bD_i} and f_{bA_j} are represented by the Fermi functions

$$\mathbf{f_{b_{D,i}}} = \frac{1}{1+\exp\left(\frac{E_F - E}{kT}\right)} \tag{2.1.2.1s}$$

and

$$\mathbf{f_{b_{A,j}}} = \frac{1}{1+\exp\left(\frac{E - E_F}{kT}\right)} \tag{2.1.2.1t}$$

Once again, under bias the above two expressions must be modified. Under voltage bias, light bias, or both the occupation probabilities are determined by the kinetics of electron capture and emission and hole capture and emission. Using the Shockley-Read-Hall model for these processes, and assuming that a donor-like banded gap state of energy between E and E+dE falling within the band $E_{2i}-E_{1i}$ in the gap only communicates with the conduction band and the valence band, allows us to write [1]

$$\mathbf{f_{b_{D,i}}} = \frac{\sigma_{pbD_i}\cdot p + \sigma_{nbD_i}\cdot\gamma_{n_i}\cdot n1_i}{\sigma_{nbD_i}(n+\gamma_{n_i}\cdot n1_i) + \sigma_{pbD_i}(p+\gamma_{p_i}\cdot p1_i)} \tag{2.1.2.1u}$$

for the i^{th} banded donor-like gap state. The corresponding expression for the j^{th} banded acceptor-like gap state of energy between E and E+dE is

$$\mathbf{f_{b_{A,j}}} = \frac{\sigma_{nbA_i}\cdot n + \sigma_{pbA_j}\cdot\gamma_{p_j}\cdot p1_j}{\sigma_{nbA_j}(n+\gamma_{n_j}\cdot n1_j) + \sigma_{pdA_i}(p+\gamma_{p_j}\cdot p1_i)} \tag{2.1.2.1v}$$

In these expressions $\sigma_{nbD_i}(E)$ and $\sigma_{pbD_i}(E)$ are the capture cross sections for electrons and holes of the i^{th} donor-like band, respectively, $\sigma_{nbA_j}(E)$ and $\sigma_{pbA_j}(E)$ are the capture cross section for electrons and holes of the j^{th} acceptor like band, and $n_{1_k}(E)$ and $p_{1_k}(E)$ are the S-R-H parameters that can be expressed as

$$n_{1_k}(E) = N_C \exp\left(\frac{E-E_C}{kT}\right) \qquad (2.1.2.1w)$$

$$p_{1_k}(E) = N_V \exp\left(\frac{E_V-E}{kT}\right) \qquad (2.1.2.1x)$$

2.1.2.1c Generalized Dopant Level Distributions

As indicated earlier, AMPS is capable of modeling any dopant gap state density of states distribution N(E) that the user desires. This is accomplished by piecing as many banded and discrete doping levels together as is necessary to represent N(E). Figure 2-4. illustrates a generalized distribution. N_D^+ and N_A^-, as appropriate, are calculated as discussed above with each "rectangle" used in the general distribution having the energy width and kinetic features (cross-sections for communication with bands) specified by the user.

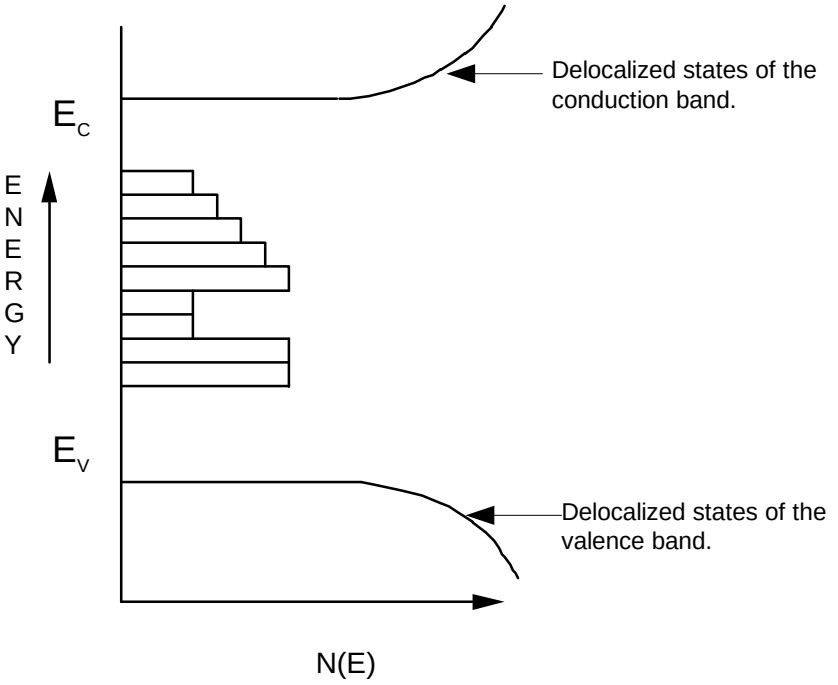

Figure 2-4. Density of states plot representing a generalized distribution of dopant states.

2.1.2.2 Defect (Structural and Impurity) Levels (n_t and p_t)

We reiterate that we break gap states into those that are purposefully present (dopant states) and those that are inadvertently present (defect states). We now consider the latter category and examine how AMPS determines n_t and p_t residing in these defect levels.

These states can be donor-like or acceptor-like, discrete and/or banded just like the dopant states of the previous section and they can be distributed across the whole bandgap. In addition, they can also be described by discrete levels and bands. AMPS also allows for continuous exponential, Gaussian, or constant distributions across the band-gap for defect states. In any case, the total charge arising in these states can be represented by

$$p_t = p_{d_t} + p_{b_t} + p_{c_t} \qquad (2.1.2.2a)$$

for the donor-like states and

$$n_t = n_{d_t} + n_{b_t} + n_{c_t} \qquad (2.1.2.2b)$$

for the acceptor-like states. Here, the p_t and n_t seen in Poisson's equation (Equation 2.1), are the total charges arising from the discrete, banded, and continuous defect (structural or impurity) energy levels. In these equations, n_{d_t} and p_{d_t} represent the total charge, originating respectively from discrete acceptor and donor concentrations, while n_{b_t} and p_{b_t}, respectively, represent the total charge developed by any banded acceptor and donor concentrations. Finally, n_{c_t} and p_{c_t}, respectively represent the total charge developed by any continuous (exponential, Gaussian, or constant) acceptor and donor concentrations. In the case of the donor-like states, Poisson's equation shows that we need the number of these states per volume that have lost an electron or, equivalently, have trapped a hole. For acceptor-like states, Poisson's equation shows that we need the number of these states per volume that have trapped an electron.

2.1.2.2a Discrete and Banded Defect (Structural and Impurity) Levels

The populations of discrete and banded defect levels arising from structural and/or impurity causes are computed identically to the computation performed on discrete and banded dopant levels. This computation has been outlined in Sections 2.1.2.1a and 2.1.2.1b. We stress, however, that AMPS distinguishes between discrete and banded defect levels and discrete and banded doping levels in the input, for the user's convenience. Chapter 3 will further explore this versatility.

2.1.2.2b Generalized Defect (Structural and Impurity) Level Distributions

The number of trapped holes per volume p_{c_t} in continuous donor-like defect states is given by

$$p_{c_t} = \int_{E_V}^{E_C} g_{D_c}(E) f_{D_c}(E) dE \qquad (2.1.2.2c)$$

where $g_D(E)$ is the continuous distribution function or density of states per unit volume per unit energy for the energy E in the gap. The quantity $f_D(E)$ is the probability that a hole occupies a state located at energy E. In thermodynamic equilibrium $f_D(E)$ is given by the Fermi function in Equation 2.1.2.1s - with the exception that the subscript i must be removed - whereas in non-thermodynamic equilibrium (situations of voltage bias or light bias), it is given by Equation 2.1.2.1u (with i removed).

The number of trapped electrons per volume n_{t_c} in these continuous acceptor-like defect states is given by

$$n_{t_c} = \int_{E_V}^{E_C} g_{A_c}(E) f_{A_c}(E) dE \qquad (2.1.2.2d)$$

where $g_{A_c}(E)$ is the distribution or density of these acceptor-like states per unit volume per unit energy for the energy E in the gap. The quantity $f_{A_c}(E)$ is the probability that an electron occupies a state located at energy E. In thermodynamic equilibrium, $f_{A_c}(E)$ is given by Equation 2.1.2.1t whereas in non-thermodynamic equilibrium $f_{A_c}(E)$ is given by Equation 2.1.2.1v (provided the subscript i removed from both equations). As noted earlier, the functions of $g_D(E)$ in Equation 2.1.2.2c and $g_A(E)$ in Equation 2.1.2.2d can be exponential, Gaussians or simply a constant. The exponentials can be either acceptor-like tails coming out of the conduction band or donor-like tails coming out of the valence band. The constant distribution can be of donor-like states from E_V to some energy E_{DA} and of acceptor-like states (of another constant value) from E_{DA} to E_t. Chapter 3 will continue discussion of these possibilities.

2.2 The Continuity Equations

Section 2.1 has provided expressions for all the quantities contributing to the charge in Poisson's equation. A close inspection of these expressions shows that they all are ultimately defined in terms of the free carrier populations n and p. We now need more information on n and p to determine how they change across a device and under different biases. The equations that keep track of the conduction band electrons and valence band holes are the continuity equations. In steady state, the time rate of change of the free carrier concentrations is equal to zero. As a result, the continuity equation for the free electrons in the delocalized states of the conduction band has the form

$$\frac{1}{q}\left(\frac{dJ_n}{dx}\right) = -G_{op}(x) + R(x) \qquad (2.2a)$$

and the continuity equation for the free holes in the delocalized states of the valence band has the form

$$\frac{1}{q}\left(\frac{dJ_p}{dx}\right) = G_{op}(x) - R(x) \qquad (2.2b)$$

where J_n and J_p are, respectively, the electron and hole current densities. The term R(x) is the net recombination rate resulting from band-to-band (direct) recombination and S-R-H (indirect) recombination traffic through gap states. Band-to-band recombination will be discussed in Section 2.2.2.1 and S-R-H recombination in Section 2.2.2.2. Since AMPS has the flexibility to analyze device structures which are under light bias (solar cells, photodetectors) as well as voltage bias, the continuity equations include the term $G_{op}(x)$ which is the optical generation rate as a function of x due to externally imposed illumination. This is discussed in Section 2.2.3.

2.2.1 Electron and Hole Current Density

Once again, we must develop expressions for the terms in a key equation. Before it was Poisson's equation; now it is the two continuity equations. Turning to J_n and J_p , we first note that transport

theory allows that, even in cases where the electron population may be degenerate or the material properties may vary with position, the electron current density J_n can always be expressed as [1]

$$J_n(x) = q\mu_n n\left(\frac{dEf_n}{dx}\right) \qquad (2.2.1a)$$

where μ_n is the electron mobility and n is defined in Equation 2.1.1a.

Similarly, even in cases where the hole populations may be degenerate or the material properties may vary with position, the hole current density still may always simply be expressed by [1]

$$J_p(x) = q\mu_p p\left(\frac{dEf_p}{dx}\right) \qquad (2.2.1b)$$

where μ_p is the hole mobility and p is defined in equation 2.1.1b. It is important to note that Equations 2.2.1a and 2.2.1b are very general formulations that include diffusion, drift, and motion due to effective fields arising from band gap, electron affinity, and densities-of-states gradients [1]. Therefore, as noted earlier, AMPS is formulated to handle structures with varying material properties including graded structures and heterojunctions.

2.2.2 The Recombination Mechanisms

There are two basic processes by which electrons and holes may recombine with each other. In the first process, electrons in the conduction band make direct transitions to vacant states in the valence band. This process is labeled as band-to-band or *direct recombination* R_D (also known as intrinsic recombination). In the second process, electrons and holes recombine through intermediate gap states known as *recombination centers*. This process, originally investigated by Shockley, Read, and Hall, is labeled *indirect recombination* R_I or S-R-H recombination (also known as extrinsic recombination). The model used in AMPS for the net recombination term R(x) in the continuity equations takes both of these processes into consideration such that

$$R(x) = R_D(x) + R_I(x) \qquad (2.2.2a)$$

The sections to follow will discuss these two processes and their mathematical representations.

2.2.2.1 Direct (Band-to-band) Recombination

The model used in AMPS for direct or band-to-band recombination $R_D(x)$ assumes that, since this recombination process involves both the occupied states in the conduction band and the vacant states in the valence band, the total rate of recombination is given by [1]

$$R = \beta np \qquad (2.2.2.1a)$$

where β is a proportionality constant which depends on the energy-band structure of the material under analysis, and n and p are the band carrier concentrations present when devices are subjected to a voltage bias, light bias, or both (see section 2.1.1). Under thermal equilibrium, the generation rate must equal the recombination rate; that is

$$R_{th} = G_{th} = \beta n_o p_o \qquad (2.2.2.1b)$$

where, again, β is a proportionality constant. The no and po factors are the carrier concentrations in thermodynamic equilibrium, expressed by Equations 2.1.1a and b. The net direct recombination rate is equal to the difference of equations 2.2.2.1a and b; that is

$$R_D(x) = R - G_{th} = \beta(np - n_o p_o) = \beta(np - n_i^2) \qquad (2.2.2.1c)$$

2.2.2.2 Indirect (Shockley-Read-Hall) Recombination

The model used in AMPS for indirect recombination $R_I(x)$ assumes that the traffic back and forth between the delocalized bands and the various types of localized gap states is controlled by Shockley-Read-Hall (S-R-H), capture and emission mechanisms. This S-R-H recombination model allows $R_I(x)$ to be expressed as [1]

$$\begin{aligned}
R_I(x) = (np-n_i^2) \Bigg\{ & \sum_i \left[\frac{N_{dD_i}\sigma_{ndD_i}\sigma_{pdD_i}\nu_{th}}{\sigma_{ndD_i}(n+n_1(E_i))+\sigma_{pdD_i}(p+p_1(E_i))} + \frac{N_{bD_i}}{W_{D_i}} \int_{E_{1i}}^{E_{2i}} \frac{\sigma_{nbD_i}\sigma_{pbD_i}\nu_{th}dE}{\sigma_{nbD_i}(n+n_1(E))+\sigma_{pbD_i}(p+p_1(E))} \right] \\
& + \sum_j \left[\frac{N_{dA_j}\sigma_{ndA_j}\sigma_{pdA_j}\nu_{th}}{\sigma_{ndA_j}(n+n_1(E_j))+\sigma_{pdA_j}(p+p_1(E_j))} + \frac{N_{bA_j}}{W_{A_j}} \int_{E_{1j}}^{E_{jj}} \frac{\sigma_{nbA_j}\sigma_{pbA_j}\nu_{th}dE}{\sigma_{nbA_j}(n+n_1(E))+\sigma_{pbA_j}(p+p_j(E))} \right] \\
& + \sum_i \left[\frac{n_{dD_{t_i}}\sigma_{ndD_i}\sigma_{pdD_i}\nu_{th}}{\sigma_{ndD_i}(n+n_1(E_i))+\sigma_{pdD_i}(p+p_1(E_i))} + \frac{n_{bD_{t_i}}}{W_{D_{ti}}} \int_{E_{1i}}^{E_{2i}} \frac{\sigma_{nbD_i}\sigma_{pbD_i}\nu_{th}dE}{\sigma_{nbD_i}(n+n_1(E))+\sigma_{pbD_i}(p+p_1(E))} \right] \\
& + \sum_j \left[\frac{n_{dA_{t_j}}\sigma_{ndA_j}\sigma_{pdA_j}\nu_{th}}{\sigma_{ndA_j}(n+n_1(E_j))+\sigma_{pdA_j}(p+p_1(E_j))} + \frac{n_{bA_{t_j}}}{W_{A_{t_j}}} \int_{E_{1j}}^{E_{2j}} \frac{\sigma_{nbA_j}\sigma_{pbA_j}\nu_{th}dE}{\sigma_{nbA_j}(n+n_1(E))+\sigma_{pbA_j}(p+p_1(E))} \right] \\
& + \int_{E_V}^{E_C} \frac{g_D(E)\sigma_{n_{CD}}\sigma_{p_{CD}}\nu_{th}\,dE}{\sigma_{n_{CD}}(n+n_1(E))+\sigma_{p_{CD}}(p+p_1(E))} + \int_{E_v}^{E_C} \frac{g_A(E)\sigma_{n_{CA}}\sigma_{p_{CA}}\nu_{th}\,dE}{\sigma_{n_{CA}}(n+n_1(E))+\sigma_{p_{CA}}(p+p_1(E))} \Bigg\} \qquad (2.2.2.2a)
\end{aligned}$$

Here the first two terms on the right-hand-side account for S-R-H traffic through discrete and banded donor dopant levels. The second two terms give the corresponding quantities for discrete and banded acceptor-dopant levels. The next two terms give the S-R-H recombination traffic through discrete and banded defect levels that are donor-like. The next two terms give the corresponding quantity for discrete and banded defect levels that are acceptor-like. The final two terms give the S-R-H contributions coming from donor and acceptor-like states that can be described by the exponential, Gaussian, or constant distributions available.

2.2.3 Optical Generation Rate

AMPS is formulated to fully analyze the behavior of any device structure subjected to bias, illumination, or both. In this section we discuss how illumination is handled by AMPS. We begin by noting that, when a semiconductor is subjected to an external source of illumination and $h\nu$ is greater than some threshold $E_{g_{op}}$ at some point x (termed the optical bandgap at x), free electron-hole pairs are produced. This is the process encompassed by the term $G_{op}(x)$ in the continuity equation of 2.2a and 2.2b. We now assume that a structure illuminated by a light source of frequency ν_i with a photon flux of $\Phi_{oi}(\nu_i)$ (in units of photons per unit area per unit time) has photons obeying $h\nu \geq E_{gop}$. This photon flux $\Phi_{oi}(\nu_i)$ is impinging at $x=0^-$(see the example of Fig 2.1). As the photon flux travels through the structure, the rate at which electron-hole pairs are generated is proportional to the rate at which the photon flux decreases. Therefore, the optical generation rate can be expressed as

$$G_{op}(x) = \frac{-d}{dx}\sum_i \Phi_i^{FOR}(\nu_i) + \frac{d}{dx}\sum_i \Phi_i^{REV}(\nu_i) \qquad (2.2.3a)$$

where $\Phi_i^{FOR}(\nu_i)$ represents the photon flux of frequency ν_i at some point x which is moving left to right in Fig 2-5 and $\Phi_i^{REV}(\nu_i)$ represents the photon flux of frequency ν_i at some point x which is moving right to left in Fig 2-5.

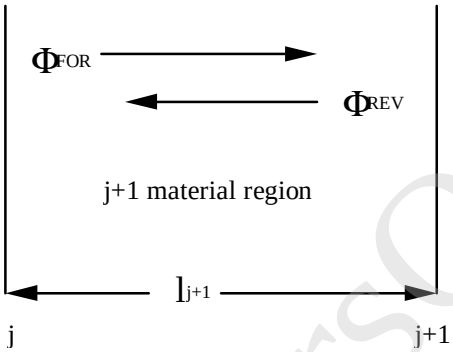

Figure 2-5. This figure illustrates the photon flux at some point x moving to the left and the photon flux at some point x moving to the right in the j+1 material region.[1]

Both $\Phi_i^{FOR}(\nu_i)$ and $\Phi_i^{REV}(\nu_i)$ exist in the device since some part of the $\Phi_{oi}(\nu_i)$ impinging at $x=0^-$ reaches the back surface and reflects. Since there may be some distribution of frequencies each with an $\Phi_{oi}(\nu_i)$ value, Equation 2.2.3a must contain a sum (in frequency) over the incoming spectrum of light as shown.

If a device has optical properties that do not vary across the structure then, at some general point x, we have

$$\Phi_i^{FOR}(\nu_i) = \Phi_{oi}(\nu_i)\bullet\{\exp[-\alpha(\nu_i)x] + R_F R_B[\exp(-\alpha(\nu_i)L)]^2 \bullet \exp[-\alpha(\nu_i)x] + \ldots\} \qquad (2.2.3b)$$

[1] It is noted that these are material layers with different properties as inputted by the user. They should not be confused with the layers defined by the mathematical grid implemented by the solution scheme. See Section 2.3.1.

whereas

$$\Phi_i^{REV}(\nu_i) = R_B\Phi_{oi}(\nu_i)\bullet\{\exp[-\alpha(\nu_i)L]\bullet\exp[-\alpha(\nu_i)(L-x)] + R_FR_B[\exp(-\alpha(\nu_i)L)]^3\bullet\exp[-\alpha(\nu_i)(L-x)] + \ldots\} \quad (2.2.3c)$$

In these expressions R_F is the reflection coefficient for the internal surface at x=0 and R_B is the reflection coefficient for the internal surface at x=L (the back surface). All of these reflection coefficients can be functions of the frequency ν_i. Any reflection and loss that may occur before x=0 (such as that at any air/glass and that in any transparent conductive oxide layer) must be accounted fro a priori by the user appropriately adjusting $\Phi_{oi}(\nu_i)$.

AMPS, of course, allows for more general situations than those covered by Equations 2.2.3b and c. Specifically, AMPS allows for the very general situation where the device structure can be made up of N regions each with its own set of optical properties (relative dielectric constant ε, absorption coefficient α for each wavelength, and index of refraction n). The $(j+1)^{\underline{th}}$ such region, of width l_{j+1} is shown in Fig. 2-6.

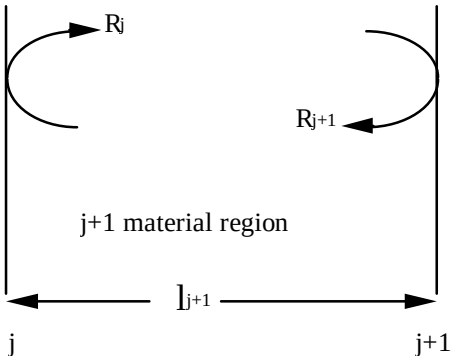

Figure 2-6. This figure illustrates the reflection of the photon flux at the j+1 boundary and at the j boundary of the j+1 region.

As this figure shows, we now have to consider reflection at the j - boundary and at the j+1 - boundary of such a region. The reflection coefficient R_j at the j - boundary can be written as [5]

$$R_j = \left\{\frac{\left[\left(\frac{\varepsilon_{j-1}}{\varepsilon_j}\right)^{1/2} - 1\right]}{\left[\left(\frac{\varepsilon_{j-1}}{\varepsilon_j}\right)^{1/2} + 1\right]}\right\}^2 \quad (2..2.3d)$$

and the reflection coefficient R_{j+1} at the j+1 - boundary can be written as

$$R_{j+1} = \left\{\frac{\left[\left(\frac{\varepsilon_{j+1}}{\varepsilon_j}\right)^{1/2} - 1\right]}{\left[\left(\frac{\varepsilon_{j+1}}{\varepsilon_j}\right)^{1/2} + 1\right]}\right\}^2 \quad (2.2.3e)$$

where the epsilons are the relative dielectric constants of each material. These reflection coefficients for the boundaries which may exist internally in a device structure can be functions of the frequency ν_i.

With these definitions for the internal reflection coefficients for the j+1 material region the quantities $\Phi_i^{FOR}(\nu_i)$ and $\Phi_i^{REV}(\nu_i)$ needed in Equation 2.2.3a for $G_{op}(x)$ can be written for every layer of any general material structure.[2]

As outlined in Appendix A, the result for the j+1 material layer is

$$\Phi_i^{FOR}(\nu_i) = \Phi_j^{LR}\{1 + R_jR_{j+1}[\exp(-\alpha_{j+1}l_{j+1})]^2 + \ldots\}\exp[-\alpha_{j+1}(x-x_j)] + R_j\Phi_{j+1}^{RL}\{\exp(-\alpha_{j+1}l_{j+1}) + R_jR_{j+1}[\exp(-\alpha_{j+1}l_{j+1})]^3 + \ldots\}\exp[-\alpha_{j+1}(x-x_j)] \quad (2.2.3f)$$

Similarly, for the j+1 material layer

$$\Phi_i^{REV}(\nu_i) = \Phi_{j+1}^{RL}\{1 + R_jR_{j+1}[\exp(-\alpha_{j+1}l_{j+1})]^2 + \ldots\}\exp[-\alpha_{j+1}(x_{j+1}-x)] + R_{j+1}\Phi_j^{LR}\{\exp(-\alpha_{j+1}l_{j+1}) + R_jR_{j+1}[\exp(-\alpha_{j+1}l_{j+1})]^3 + \ldots\}\exp[-\alpha_{j+1}(x_{j+1}-x)] \quad (2.2.3g)$$

By using expressions like these for every layer of material and by matching the flux at each boundary, the set of terms Φ_j^{LR} and Φ_j^{RL} appearing in these equations can all be determined. As outlined in Appendix A, AMPS consistently obtains all these Φ_j^{LR} and Φ_j^{RL} terms for each frequency ν_i allowing it to completely specify Equations 2.2.3f and g for each material region and for each frequency ν_i. This allows Equation 2.2.3a to be completely determined and available for use in the continuity equations (Equation 2.2a and 2.2b).

2.2.4 Boundary Conditions

The three governing equations (2.1), (2.2a), and (2.2b) must hold at every position in a device and the solution to these equations involves determining the state variables $\Psi(x)$, $E_{Fn}(x)$, and $E_{fp}(x)$ or, equivalently, $\Psi(x)$, n(x), and p(x) which completely defines the system at every point x. Because the governing equations for $\Psi(x)$, $E_{Fn}(x)$, and $E_{Fp}(x)$ (or, equivalently, $\Psi(x)$, n(x), and p(x)) are non-linear and coupled, they cannot be solved analytically. Hence, numerical methods must be utilized. Section 2.3 discusses the Newton-Raphson technique, which is used in AMPS and AMPS to numerically solve the resulting algebraic equations. Like any other mathematical analysis, there must be boundary conditions imposed on the set of equations. These are expressed in terms of conditions on the local vacuum level and the currents at the contacts. To be specific the solutions to equations (2.1), (2.2a), and (2.2b) must satisfy the following boundary conditions:

$$\Psi(0) = \Psi_o - V \quad (2.2.4a)$$

$$\Psi(L) = 0 \quad (2.2.4b)$$

$$J_{p(0)} = -qS_{po}(p_o(0) - p(0)) \quad (2.2.4c)$$

[2] It is noted that these are material layers with different properties as inputted by the user. They should not be confused with the layers defined by the mathematical grid implemented by the solution scheme. See Section 2.3.1.

$$J_{p(L)} = qS_{pL}(p(L) - p_o(L)) \quad (2.2.4d)$$

$$J_{n(0)} = qS_{no}(n(0) - n_o(0)) \quad (2.2.4e)$$

$$J_{n(L)} = -qS_{nL}(n_o(L) - n(L)) \quad (2.2.4f)$$

where x=0 refers to the left-hand side and x=L to the right-hand side of any general device structure under consideration.

In boundary conditions 2.2.4a and 2.2.4b the quantities $\Psi(0)$ and $\Psi(L)$ are the function Ψ in Equation 2.1 evaluated at x=0 and x=L in. We restate that $\Psi(x)$ is, in general, the energy difference between the local vacuum level at point x and its value at the contact on the right hand side of any device structure (see Figure 2-1). Its value at x=0 in thermodynamic equilibrium is Ψ_o, and using our definition its value is zero in thermodynamic equilibrium at x=L. In fact $\Psi(L)$ is always zero no matter what the light or voltage condition because of our choice of reference for Ψ. However, $\Psi(0)$ becomes Ψ_o-V if a voltage bias, light bias, or both exist. Here V is taken as positive if the Fermi level in the right contact (at x=L) is raised by V above the Fermi level at the left contact (x=L). All of this leads to conditions described by Equations 2.2.4a and 2.2.4b which are valid for all structures for all situations.

We summarize by noting that in thermodynamic equilibrium Equation 2.2.4a shows that $\Psi(0)=\Psi_o(0)$ whereas Equation 2.2.4b shows that $\Psi(L)=0$. If a voltage V develops between the contact at x<0 and the contact at x>L, $\Psi(L)$ does not change but $\Psi(0)$ does change with respect to the local vacuum level in the right hand contact and the amount of this change is V. In AMPS we adopt the convention that, if the contact at x<0 is positive with respect to the contact at x>L, then V is taken as positive. We reiterate that, under any bias $\Psi(0) = \Psi_0(0)$-V which, as seen, is boundary condition 2.2.4a and $\Psi(L)=0$ which, as seen, is boundary condition 2.2.4b.

In boundary condition statements 2.2.4c-2.2.4f $p_0(0)$ and $p_0(L)$ are the valence band hole populations at x=0 and x=L, respectively, in thermodynamic equilibrium whereas $n_0(0)$ and $n_0(L)$ are the conduction band electron populations at x=0 and x=L, respectively, in thermodynamic equilibrium. The quantities p(0) and p(L) are the corresponding hole populations, under operating conditions, at x=0 and at x=L, respectively. The quantities n(0) and n(L) are the corresponding electron populations, under operating conditions, at x=0 and at x=L, respectively. The quantities S_{p0},S_{pL},S_{n0}, and S_{nL}, appearing in conditions 2.2.4c-2.2.4f are effective surface recombination speeds for holes at x=0 and x=L, respectively, and for electrons at x=0 and x=L, respectively. We will comment on these quantities shortly. Conditions 2..2.4c-2.2.4f must be matched by equations 2.2.1a and 2.2.1b at x=0 and x=L under operating conditions. Under thermodynamic equilibrium conditions 2.2.4c-2.2.4f are identically equal to zero.

At this point we make two additional comments on the boundary condition approach used in AMPS. First we note that, although we called the S quantities in equations 2.2.4c-2.2.4f effective surface recombination speeds, these equations do not limit the transport mechanisms at the boundaries to surface recombination. With this general formulation of 2.2.4c-2.2.4f the transport in each of these four statements could be recombination [1] or thermionic emission depending on the value of S which is chosen. For example, if S_{p0}, is taken to be the thermal velocity for holes, then the holes are crossing x=0 by thermionic emission. If a value of S is chosen to represent surface recombination, the value selected can be used to reflect the degree of surface passivation.

This freedom in choosing S (and the barrier height at x=0 and x=L which is documented in Section 3.3) also means one has freedom in choosing the degree of ohmicity at a contact. Obviously, to have an ideal ohmic contact at x=L for electrons, for example, one has to select S_{nL} large enough to insure that $n(L)=n_0(L)$ for all biasing conditions that are to be considered. This follows from Equation 2.2.4f.

To try to further convey how versatile the treatment of boundaries in AMPS we consider a case in which current is flowing at a boundary by recombination but the user wishes to account for surface recombination speeds that may vary with carrier populations, currents, and bias. To gain this extra flexibility one simply chooses low S values for the boundary where this is to occur. Adjacent to this boundary one then defines a surface region, with a specified gap state distribution and its concomitant capture cross-section values. With S chosen low enough, it is insured that current flow will be controlled by recombination in the surface layer created by the user. This surface region thus can be chosen to control recombination at the boundary. This recombination will be described with the full S-R-H formulation described previously in section 2.2.2.

2.3 Solution Techniques

We have now developed all the equations needed to analyze transport phenomena in a wide variety of device types and biasing situations. These equations are obviously both highly non-linear and coupled. Due to this non-linearity and coupling, numerical methods are necessary to obtain a solution. Because of the discrete nature of these solution techniques, the definition domain of our equations must also be discretized. This section will detail our approach to implementing this discretization scheme and we hope to familiarize the reader with the numerical solution techniques used by AMPS. To better explain our approach to solving the set of three coupled non-linear differential equations, we will divide this section into three parts. First, our approach to discretizing the definition domain of the dependent variables will be defined. Next, the discretization of the differential equations through the method of finite differences will be discussed. Lastly, a discussion of the numerical algorithm used by AMPS to solve the set of discretized equations will be presented.

2.3.1 Discretization of the Definition Domain

The definition domain in AMPS is the region $0 \le x \le L$. The device exists in this region is defined solely by the user. It clearly can be a very general microelectronic or photonic structure. Once it is defined, AMPS breaks the structure down into N slabs and N+1 major grid points (see Fig. 2-1).

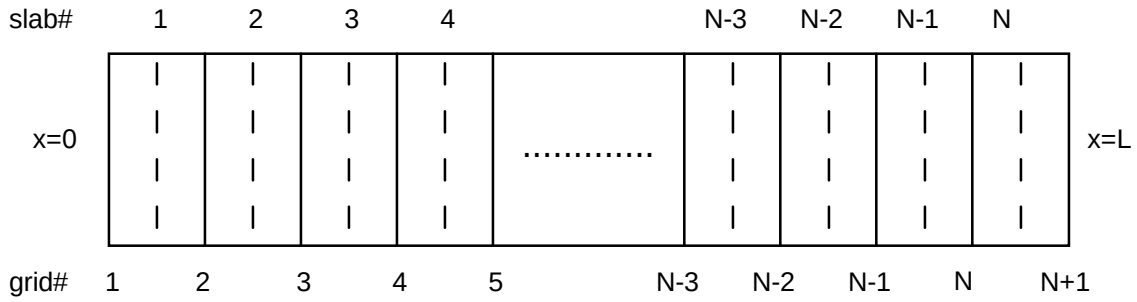

Figure 2-7. A grid used in numerical methods. There are N slabs (dashed lines) and N+1 major grid points (solid lines). The example shown here is a uniform grid.

The major grid points, represented by the solid lines, are the points in the device for which the unknowns, Ψ, E_{Fp}, and E_{Fn} are solved. The minor grid points, represented by the dashed lines, are the points in the device for which the current densities are formulated using the Scharfetter-Gummel approach which will be discussed in Section 2.3.2. [4]. A non-uniform grid spacing is usually adopted such that the spacing is decreased in regions where the dependent state variables change more rapidly. This is at the discretion of the user. (see Chapters. 3 and 4)

2.3.2 Discretization of the Differential Equations

To discretize the differential equations the method of finite differences is utilized [5]. This method replaces the differential operators with difference operators. For example, the second derivative of the vacuum level in Poisson's equation is represented by finite central differences. In this manner,

$$\frac{d^2\Psi(x_i)}{dx^2} = \frac{\Psi x_{i+1} - 2\Psi x_i + \Psi x_{i-1}}{h+H} \tag{2.3.2a}$$

where h is the backward distance between adjacent grid points and H is the forward distance between adjacent grid points in the device. AMPS allows for the fact that these distances may be different if a variable grid size is implemented by the user.

In the continuity equations the derivative terms are the derivatives of the current densities. Typically, the current densities for holes and electrons are given by equation 2.2.1a and b. However, if those expressions are used for the current densities, and their derivatives are expressed as differences, numerical methods have extreme difficulty converging to a solution. To avoid this problem, Scharfetter and Gummel derived a so-called trial function representation for J_n and J_p that allows their derivatives to be more amenable to numerical methods [3]. These derivatives are represented by

$$\left[\frac{dJ_p}{dx}\right]_i = \frac{J_{p_{i+1/2}} - J_{p_{i-1/2}}}{h+H} \tag{2.3.2a}$$

for the hole continuity equation and

$$\left[\frac{dJ_n}{dx}\right]_i = \frac{J_{n_{i+1/2}} + J_{n_{i-1/2}}}{h+H} \tag{2.3.2b}$$

for the electron continuity equation where trial functions are used for the current densities J_n and J_p in Equations 2.3.2a and 2.3.2b. The trial function for J_n, derived in Appendix B, is given by

$$J_{n,i+1/2} = \frac{\left[\frac{qkT\mu_n N_c \exp\left(\frac{-\phi_{bL}}{kT}\right)}{H}\right]\left[\exp\left(\frac{E_{fn_{i+1}}}{kT}\right) - \exp\left(\frac{E_{fn_i}}{kT}\right)\right]\left[\frac{\Psi_{i+1}}{kT} - \frac{\Psi_i}{kT}\right]}{\left[\exp\left(\frac{\Psi_{i+1}}{kT}\right) - \exp\left(\frac{\Psi_i}{kT}\right)\right]} \tag{2.3.2b}$$

and the trial function for J_p, also derived in Appendix B, is given by

$$J_{p,i+1/2} = \frac{\left[\frac{qkT\mu_p N_v \exp\left(\frac{-\phi_{bL} - E_G}{kT}\right)}{H}\right]\left[\exp\left(\frac{E_{fp_{i+1}}}{kT}\right) - \exp\left(\frac{E_{fp_i}}{kT}\right)\right]\left[\frac{\Psi_{i+1}}{kT} - \frac{\Psi_i}{kT}\right]}{\left[\exp\left(\frac{-\Psi_{i+1}}{kT}\right) - \exp\left(\frac{-\Psi_i}{kT}\right)\right]} \qquad (2.3.2c)$$

By replacing i+1 with I-1 and H with h and by placing a negative sign in front of the entire equation, similar expressions can be written for $J_{n,i-1/2}$ and $J_{p,i-1/2}$.

With this discretization of the derivatives in Poisson's equation and in the two continuity equations, these equations may be recast as three functions f_i, f_{ei}, and f_{hi} and expressed in difference form. The equation for f_i, which corresponds to Poisson's equation, is

$$f_i(\Psi^*_{i-1},\Psi^*_i,\Psi^*_{i+1}) = -(A^*_{i-1}\Psi^*_{i-1} - A^*_i\Psi^*_i + A^*_{i+1}\Psi^*_{i+1}) + \rho_i(\Psi^*_i) \qquad (2.3.2d)$$

This represents having all the terms in Poisson's equation at grid point "i" written on the right hand side and expressed in terms of the nondimensionalized variable $\Psi^*=\Psi/kT$. The three "A" prefactors seen in Equation 2.3.2d are given by

$$A^*_{i-1} = \frac{4\varepsilon_i\varepsilon_{i-1}kT}{h(h+H)(\varepsilon_i+\varepsilon_{i-1})}, \qquad (2.3.2e)$$

$$A^*_{i+1} = \frac{4\varepsilon_i\varepsilon_{i+1}kT}{H(h+H)(\varepsilon_i+\varepsilon_{i+1})}, \qquad (2.3.2f)$$

and

$$A^*_i = A^*_{i-1} + A^*_{i+1} \qquad (2.3.2g)$$

where $A^*_i = kT*A_i$. The function f_{ei}, corresponding to the electron continuity equation written at point i, is given by

$$f_{e_i}(x) = \frac{2}{q(h+H)}[J_{n,i+1/2}(x) - J_{n,i-1/2}(x)] + G_{op,i}(x) - R_i(x) \qquad (2.3.2h)$$

and the function f_{hi}, corresponding to the hole continuity equation written at the point i, is given by

$$f_{h_i}(x) = -\frac{2}{q(h+H)}[J_{p,i+1/2}(x) - J_{p,i-1/2}(x)] + G_{op,i}(x) - R_i(x) \qquad (2.3.2i)$$

In these equations G_{op} and R are given, respectively, by Equations 2.2.2a and 2.2.3a.

There are N-1 sets of these equations (a set at every interior grid point in the device of Fig. 2-7). In addition there are six boundary conditions from Equations 2.2.4a-2.2.4f. This gives a total of 3N+3 equations that must be solved by AMPS. Solving means finding the values of Ψ, E_{Fn}, and E_{Fp} (the roots) in the right had sides of Equations 2.3.2d, 2.3.2h, and 2.3.2i that makes the left hand side zero at every grid point. We note that the J_n and J_p given by the Scharfetter-Gummel trial function is also used in the expressions from Equations 2.2.4c-2.2.4f when setting up the boundary conditions.

2.3.3 Newton-Raphson Method

The Newton-Raphson Method is used in AMPS to solve this set of 3(N+1) algebraic equations resulting from breaking a device structure into N slabs and from writing the governing differential equations in terms of differences in the state variables Ψ, E_{Fn} and E_{Fp} at the grid points defining these slabs. It is a method that iteratively finds the roots of a set of functions f_i, f_{e_i}, and f_{h_i}, if given an adequate initial guess for the roots. We stress that the key to success (convergence) is having an adequate initial guess. Routines are built into AMPS to generate these initial guesses.

The Newton-Raphson technique is discussed in a number of standard texts on numerical methods [4]. For AMPS to effectively use the Newton-Raphson method the required 3(N+1) equations must be set up in an efficient matrix format. As we noted, six of these come from the boundary conditions and 3(N-1) from the discretization at the N-1 interior slab boundaries. For each of these equations the Newton-Raphson method also requires the partial derivatives with respect to the state variables Ψ,E_{Fp}, and E_{Fn} be taken at each discretization point. If we let the matrix A be the Jacobian matrix of these partial derivatives, the matrix δ be the matrix of the $\delta\Psi_i$, $\delta E_{fn,i,}$ and $\delta E_{fp,i}$ where these are the difference between the initial guess for a state variable at point i and the corrected value of the state variable at i, and B be the matrix formed by evaluating the functions f_i, f_{e_i}, and f_{h_i}, at the point i, then

$$[A]\bullet[\delta] = [B] \tag{2.3.2a}$$

The matrices A and B are initially evaluated using the initial guesses for the state variables. They are subsequently evaluated using the matrix δ to up-date the guesses as the solution evolves toward the actual values of the state variables. The matrix δ is constructed as

$$\begin{bmatrix} \Uparrow \\ \delta\,\Psi \\ \delta E_{fp_i} \\ \delta E_{fn_i} \\ \Downarrow \end{bmatrix} \tag{2.3.2b}$$

and the matrix B is constructed as

$$\begin{bmatrix} \Uparrow \\ f_i \\ f_{e_i} \\ f_{h_i} \\ \Downarrow \end{bmatrix} \tag{2.3.2c}$$

We point out that the δ and B matrices are set up in an order that allows the Jacobian matrix A to be a banded matrix of the smallest size possible. This minimizes the amount of computer time necessary to invert the matrix A to solve for the matrix δ. To solve for the matrix δ, L-U decomposition is used [4].

In using the Newton-Raphson method it is important to note that Poisson's equation and the continuity equations must be arranged so that the root may be found; *i.e.*, the equations must be arranged so that they equal zero as was discussed in Section 2.3.2. After each iteration, the matrix δ is added to the latest guess, as has been noted, until the smallest value contained within the matrix δ is less than some predetermined error criterion. In AMPS, this error criterion is equal to 10^{-6} kT for all the state variables (expressed in dimensional form) at each point. This is seen to be a very rigorous criterion.

To demonstrate the Newton-Raphson algorithm that AMPS uses, we briefly outline the step-by-step procedure. This procedure begins by first finding a solution for thermodynamic equilibrium, since only Ψ needs to be determined in that case. Therefore, Poisson's equation needs to be solved simultaneously at the N-1 points within the device while imposing the thermodynamic equilibrium boundary conditions at the two boundary points. Choosing an initial guess for the solution for Ψ to begin the Newton-Raphson technique is very important. For thermodynamic equilibrium the initial guess built into AMPS for Ψ is a straight line connecting the boundary values. Poisson's equation is evaluated at the N-1 interior points with the initial guess to generate the f_i at each point as well as the values of the partial derivatives involved in the Jacobian matrix. After solving for the matrix δ, the matrix δ is added to the initial guess and Poisson's equation and the partial derivatives are recalculated. This continues until every value of the matrix δ is less than 10^{-6}kT. When this condition is met, the initial guess for Ψ has been fully evolved to the actual Ψ at thermodynamic equilibrium in the device.

With the solution in thermodynamic equilibrium known, AMPS now is able to handle any set of voltage biases, light biases, or both called for by the user. To do so, AMPS first uses the $\Psi(x)$ calculated from thermodynamic equilibrium as a basis for formulating its initial guess to $\Psi(x)$ under the biasing. It uses a built-in routine to generate the initial guesses now needed for the other two state variables that come into play with bias present, namely, Efn(x) and Efp(x). In applying voltages, such as when AMPS steps through a dark current-voltage sweep, constant voltage steps are used. In each of these voltage steps AMPS needs new initial guesses for all the unknowns. Routines for these are built into the program.

To determine the device characteristics with a light bias applied, AMPS generates the dark current-voltage characteristics. Light, as dictated by the user, is then turned on and AMPS steps through the current-voltage characteristics under illumination.

2.4 Constructing the Full Solution

Once the state variables Ψ, E_{Fn}, and E_{Fp} are determined for a given set of biasing conditions (voltage, light, or both) and temperatures, the current density-voltage (J-V) characteristics for these conditions can be generated. The J-V characteristic for some temperature T, with or without the presence of light, is obtained from the fact that $J=J_p(x) + J_n(x)$ where x is any plane in the device and J_n and J_p are obtained from Equations 2.2.1a and 2.2.1b. Similarly the electrostatic field ξ throughout the device can be generated for the various conditions using $\xi = d\Psi/dx$ and recombination can be generated using Equation 2.2.2a. In fact all the internal "workings" going on in a device (n,n_t,p_t,etc) can be generated for a given set of conditions, as desired by the user.

CHAPTER 3
MATERIAL PARAMETERS

3.0 Introduction

Now that we have discussed in Chapter 2 the basic equations and solution techniques used in AMPS to solve for the current density-voltage-temperature (J-V-T) characteristics of a device, the recombination taking place as a function of position, temperature, voltage, etc. in a device, the various populations present throughout the device, and the other "workings" going on inside a general structure under bias, we are ready to further describe the parameterization approach used in AMPS to represent semiconductors, insulators, and metals. Parameterization of the properties of these materials are needed since they are the building blocks of all the various types of devices we are interested in designing, analyzing, and optimizing. This section, which describes in detail the material parameters needed in AMPS for these various materials, is divided into five major subsections. Subsections 3.1, 3.2, and 3.3 will describe the parameters used to represent semiconductor materials, insulating materials, and metals. Subsection 3.4 describes how AMPS parameterizes interfaces of different regions within a device and the interfaces at the contacts. AMPS also takes into consideration situations where the material parameters can vary with position. This case is described in section 3.5.

3.1 Parameters for Representing Semiconductor Properties

This subsection is an in-depth discussion of the parameters needed to represent semiconductor materials. We will assume in this subsection that we are dealing with a semiconductor layer of some thickness specified by the user. There may be just one such layer in a device or a number of such layers. Cases where semiconductor properties are continuously varying are discussed in subsection 3.5. All three different classes of semiconductor materials are modeled within AMPS; namely, crystalline material, polycrystalline material, and amorphous material. Subsections 3.1.1, 3.1.2, and 3.1.3 discuss crystalline, amorphous materials, and polycrystalline cases respectively.

3.1.1 Lifetime picture

When using this lifetime picture of recombination/thermal generation described by Eqn (3.1.1 a) and (3.1.1b) to model S-R-H or B-T-B process, there are some procedures that should be followed and a few kept in mind:

p-type $R_n=\Delta n/\tau_n$ (3.1.1a)

n-type $R_p=\Delta p/\tau_p$ (3.1.1b)

(1) In steady state operation (which is what AMPS models) Rn must always equal Rp. hence when using the linearized lifetime picture of Eqn (3.1.1a) and (3.1.1b), one must be careful not to over specify the problem.

For example, looking at Eqn (3.1.1a) and (3.1.1b), one notes that **a lifetime** value could only apply to both carriers if $n-n_0=p-p_0$. AMPS/.windows set up to give you Self-Consistancy-Check (SCC) lifetimes back at the end of a run by its calculating $\Delta n/R$ and $\Delta p/R$. So, if you believe the linearized models are good for both carriers and that there is a lifetime that applied to both carriers, then you can check the self-consistency of this by seeing if the AMPS calculated SCC lifetime are equal (equal to your inputted values). If you think the lifetime concept and the linearization of R applied to electrons, then you are assuming Eqn (3.1.1a) is valid. In this case you should not specify anything about holes. You let AMPS worry about keeping $R_n=R_p$. At the end of the run, AMPS will calculate the SCC lifetimes. If you were right initially, then the SCC electron lifetime will be equal to what you inputted. The SCC hole is meaningless in this case.

The corresponding procedure is followed if you believe the lifetime applies to holes. The key is to check that the SCC lifetime is what you inputted for holes; ie, you must check that you are being self-consistent.

In general there will be regions in real devices where one is not sure if the linearized lifetime model for electrons or the linearized lifetime model for holes is better applied. In those situations assume the lifetime applies to both carriers (ie, assume recombination can be linearized for both carriers and that the lifetime applies to both carriers) and run AMPS. Then look at the outputted SCC lifetimes. in regions where the SCC lifetimes are equal (and essentially equal to what you inputted), leave things alone. In regions where the SCC electron lifetime << hole lifetime, AMPS is telling you it makes more sense to think of the linearized model as being appropriate for electrons. It is telling you conduction band electron are the controlling carrier and hence, your inputted lifetime has to be redone as an electron lifetime. The procedure for when the SCC electron lifetime >> SCC hole lifetime is, therefore, just the opposite.

(2) The lifetime picture uses Eqn (3.1.1a) and (3.1.1b) and consequently it does not account for the details of S-R-H recombination; ie, it does not look at defect charging resulting from carriers passing through these states (This charging is overlooked since neither DOS nor capture-cross-sections are specified). This picture does not encompass, therefore, any field redistribution effects which may occur during device operation due to charge build-up in device states.

(3) Neither S-H-R nor B-T-B recombination/thermal generation are really the simple, linear processes described in Eqn (3.1.1a) and (3.1.1b). For S-R-H net recombination the trapping through each group of defects of density N_t is given by

$$R=R_n=R_p= (np-n_0p_0)/(\tau_{p0}(n+nt)+\tau_{n0}(p+p_t)) \qquad (3.1.1c)$$

where τ_{p0} and τ_{n0} are short hand for reciprocals of the thermal velocity-hole/electron capture cross section and Nt product. The quantities n_t and p_t depends exponentially on the position of the defects in the energy band gap. For B-T-B net recombination

$$R=R_n=R_p=k(np-n_0p_0) \qquad (3.1.1d)$$

where R is a constant that depends on the material and is to first order, independent of carrier populations.

Equation (3.1.1c) and (3.1.1d) made it clear that the linearized versions seen in Eqn (3.1.1a) and (3.1.1b) are only rigorously true if you are lucky. You have to be especially lucky in the case of S-R-H recombination since the carrier populations ever appear in the factors multiplying ($np-n_0p_0$).

3.1.2 DOS picture

In this version of AMPS/windows, the user has the choice of two different approaches. One is what we term the density of states (DOS) picture; the other is what we term the carrier lifetime picture.

In the DOS picture the details of recombination traffics, trapping and the charge state of the defects (and the effects of this charge on the electric field variation across a structure) are fully accounted for. Because all the recombination traffics, trapping, re-admission, etc. - and their effects on the electric field- are in the DOS picture, this approach requires that the user input the energy gap distribution of the defects as well as their spatial variation. This approach also requires capture cross section information to quantify the attractiveness of the various defects to electrons and holes. The Shockly-Read-Hall (S-R-H) model is used for the capture and emission process in this DOS approach. AMPS also uses the resulting charge in the defect state in its calculation with Possion's equation.

This DOS picture is needed when dealing with material that have significant defect densities such as amorphous silicon materials and grain boundary region of polycrystalline materials. If this DOS picture is not used, one does not account for electric field distribution changes that occurs due to charge build-up in defect states.

In the lifetime picture, the assumption is made that S-R-h or Band-To-Band (B-T-B) net recombination/thermal generation can be modeled with linear models that look like

p-type $R_n=\Delta n/\tau_n$ (3.1.2a)

n-type $R_p=\Delta p/\tau_p$ (3.1.2b)

Here Δn is the change in the conduction band electron population n from its thermodynamic equilibrium value n_0. Corresponding Δp is the change in the valance band hole population p from its thermodynamic equilibrium value p_0. The quantity τ_n is referred to as the electron lifetime and τ_p is referred to as the hole lifetime. In steady state (which is what AMPS/windows model) $R=R_n=R_p$ is always true.

3.1.2.1 Parameters for Single Crystal Semiconductor Materials

This section describes the parameters AMPS needs to tell the mathematics of Poisson's equation (Equation 2.1), the carrier transport (continuity) equations (Equations 2.2a & b), and the recombination/generation equations (Equations 2.2.2a & 2.2.3a) about the presence of a single crystal semiconductor material in some region of a device. This single crystal layer existing in some region of the device is seen in Fig. 3.1.

3.1.2.1.1 Band State Parameters

The mathematical expressions given for n=n(x), the number of electrons at some point per volume in the conduction band, and for p=p(x), the number of missing electrons at some point per volume (i.e., holes per volume) in the valence band in Equations 2.1.1a and b require band parameters for this layer of single crystal material. This may be seen by noting that, for the single crystal layer of constant material parameters seen in Fig 3.1, n from Equation 2.1.1a can be rewritten in terms of our state variables Ψ, E_{Fn}, and E_{Fp} as

$$n = N_c F_{1/2}\left[\frac{E_{Fn}-\Phi_{bL}-\chi_e(L)+\chi_e-\Psi(x)}{kT}\right] \qquad (3.1.2.1.1a)$$

$$\text{where } E_c = \Phi_{bL} + \chi_e(L) + \Psi(x)-\chi_e \qquad (3.1.2.1.1b)$$

Similarly p from Equation 2.1.1b can be rewritten as

$$p = N_v F_{1/2}\left[\frac{\Phi_{bL}+\chi_e(L)-\chi_e-E_G+\Psi(x)+E_{Fp}}{kT}\right] \qquad (3.1.2.1.1c)$$

where

$$E_v = \Phi_{bL} + \chi_e(L) -\chi_e -E_G + \Psi(x) \qquad (3.1.2.1.1d)$$

These expressions are valid for this layer for thermodynamic equilibrium, in which case $E_{Fn}=E_{Fp}=0$, since these assume E_{Fn} is measured positively up and E_{Fp} positively down from the Fermi level position in the ohmic contact at x>L.[3] They are also valid when biasing is present.

From Equations 3.1.2.1.1a and 3.1.2.1.1b, it can be shown that to specify n and p in this layer, we must give the band effective densities of states N_c and N_v for the layer, the electron affinity χ_e for the layer, and the energy gap E_G for the layer. It is also clear from these expressions that AMPS will require the barrier height at the contact at x=L as well as the electron affinity in the semiconductor adjacent to the contact at x=L.

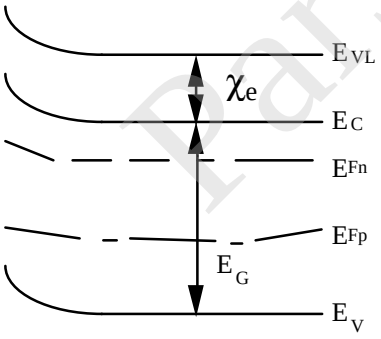

Figure 3-1 A band diagram for a layer of a device that has constant material parameters.

[3] Note that this reference is chosen because, as discussed earlier, it does not shift with respect to the vacuum level when the structure is subjected to a perturbation.

3.1.2.1.2 Localized (Gap) State Parameters

In general there may be a variety of different types of gap (i.e., localized) states existing in the energy gap of the layer seen in Fig. 3.1, even though the material is single crystal. As detailed in Chapter 2, AMPS breaks these states into two classes: those that are inadvertently present due to defects (structural and impurity) and those that are purposefully present due to doping. As we also noted, there may be donor-like and acceptor-like states among both classes.

3.1.2.1.2.1 Parameters for Doping Levels

We turn first to a survey of the parameters needed to describe doping levels in our single crystal semiconductor layer of constant material parameters. The doping levels in our usage include states which are characterized by discrete levels and states that form a band with a bandwidth defined by an upper energy boundary and a lower energy boundary. This latter case of localized gap state bands can arise if heavy doping is present in a structure as noted in Chapter. 2. It is important to note that any combination of these two unique types of states is acceptable to AMPS (see section 2.1.2.1c).

3.1.1.2.1a Parameters for Discrete Dopant Levels

Discrete dopant-caused localized sites have single energy levels and arise from the intentional introduction of impurities. For these types of states there can be up to nine donor energy levels and nine acceptor energy levels. Population in these sites is given by Equations 2.1.2.1c through 2.1.2.1n. The user has a choice of assuming full ionization or having AMPS compute the populations using Fermi-Dirac statistics for these states. If full ionization is assumed, then the donor doping concentrations of the i^{th} discrete level N_{dDj} or the acceptor doping concentrations of the j^{th} discrete level $N_{dA,j}$ are all that need to be specified and they are charged such that $N_{dD,i}^{+} = N_{dD}$ and $N_{dA,j}^{-} = N_{dA,j}$. In the fully ionized case, AMPS computes the total ionized donor states per volume N_{dD}^{+} and the total ionized acceptor states per volume N_{dA}^{-} from a summation taken over the number of energy levels (specified by the user).

In situations where the user does not insist that the dopants are all fully ionized, AMPS figures out their degree of ionization. For the discrete levels under discussion, it does so by using Equations 2.1.2.1c and d with $\mathbf{f}_{D,i}$ given by Equation 2.1.2.1g and $\mathbf{f}_{A,j}$ is given by Equation 2.1.2.1h. The n and p in these expressions are given for the constant-property semiconductor layer under discussion, by Equations 3.1.1.1a and c, respectively. These expressions, Equations 2.1.2.1c and d and Equations 2.1.2.1g and h, are valid for biasing situations and for thermodynamic equilibrium. In the latter case, the expressions for $\mathbf{f}_{D,i}$ and $\mathbf{f}_{A,j}$ pass over to the appropriate Fermi functions when the thermodynamic equilibrium values are used for n and p.

If discrete dopant states are assumed to be fully ionized, they do not participate in recombination. However, if the states are not fully ionized, then their occupation probabilities are given, in general, by $\mathbf{f}_{D,i}$ (Equation 2.1.2.1g) or $\mathbf{f}_{A,j}$ (Equation 2.1.2.1h), respectively, as was just noted. These $\mathbf{f}_{D,i}$ and $\mathbf{f}_{A,j}$ are determined by the Shockley-Read-Hall recombination traffic through the levels. These levels, therefore, contribute recombination. This contribution is embodied in the first and third terms on the right-hand side of Equation 2.2.2.2a.

From Equations 2.1.2.1c, 2.1.2.1d, 2.1.2.1g, and 2.1.2.1h and Equation 2.2.2, it can be seen that the modeling of these discrete dopant states which are not assumed to necessarily be fully ionized

demands several additional pieces of information. Now, in addition to specifying the donor or acceptor concentration $N_{dD,i}$ or N_{dD_j} for each i^{th} or j^{th} level, we must specify its location in energy from the conduction band (E_{DON_i} for donors) or its location in energy from the valence band (E_{ACP_j} for acceptors), and the capture cross-sections σ_{ndD_i}, σ_{pdD_i} (for donors), σ_{ndA_j} and σ_{pdD_j} (for acceptors) for each level.

3.1.2.1.2.1b Parameters for Banded Dopant Levels

As noted in Chapter 2, AMPS allows for the possibility that there may be dopant bands in the energy gap. Heavy doping, for example, can cause this in single crystal materials. Banded localized dopant sites are characterized by lower and upper energy boundaries. The total population in these banded dopant states is given by Equations 2.1.2.1o and p. The population in some i^{th} donor and j^{th} acceptor band is given by Equations 2.1.2.1q and r, respectively. In these expressions, the probability of occupation function is given by Equation 2.1.2.1u for donor levels and Equation 2.1.2.1v for acceptor levels. In these expressions, n is given in general by 3.1.2.1.1a and p is generated by Equation 3.1.2.1.1c. In the special case of thermodynamic equilibrium $E_{Fn}=E_{Fp}=0$ in these expressions.

Recombination through these bands of dopant states, which may be present in our single crystal layer with constant material properties, is given by the second and fourth terms on the right hand side of Equation 2.2.2.2a. This equation, Equations 2.1.2.1u and v, as well as Equations 2.1.2.1q and r, show that band dopant levels require the specification of a number of parameters. For the i^{th} such dopant band, these are seen to be the energies E_{1_i} and E_{2_i}, the concentration (N_{D_i} or N_{A_i}), and the capture cross-sections (σ_{ndD_i} and σ_{pdD_i} or σ_{ndA_j} and σ_{pdD_j}).

3.1.2.1.2.2 Parameters for Defect Levels

We now consider the charge residing in, and the recombination traffic taking place through, the localized levels arising from structural or impurity defects (see section 2.1.2.2 for the mathematical development) that may exist in the single crystal layer with constant material properties seen in Fig 3-1. These states can be donor-like or acceptor-like, discrete or banded, just like the dopant states of the previous section. AMPS also allows certain continuous functions (exponential, Gaussian, or a constant) for these states.

3.1.2.1.2.2a Parameters for Discrete and Banded Defect Levels

Populations and recombination traffic through discrete and banded defect levels are computed in a manner which is identical to the computation performed on discrete and banded dopant levels; however, AMPS does distinguish between localized states arising from defects and from doping in its input. More will be said about this in Chapters 4 and 5. Since the mathematical representation of discrete and banded dopant defect states is identical, the parameters needed to model these states are identical. To be specific, discrete defect states are described by specifying a density, energy position in the gap, and capture cross-sections for holes and electrons. Banded defect states are described by a density, by the two energies defining the width and location of the band, and by capture cross-sections for holes and electrons. Chapters 4 and 5 detail the input of this information.

3.1.2.1.2.2b Parameters for the Continuous Defect Levels

Continuous defect states are those localized states that form a continuum throughout the band gap. These continuum gap states are to be distinguished from the discrete and banded localized gap states which only exist at specific energies or at a specific range of energies in the gap. AMPS offers the possibility of three different types of continuous distributions: exponential, Gaussian, and constant distributions. The possibility of an exponential distribution of gap states is included in AMPS, because even single crystal materials, such as our layer in Fig. 3-1, are found to have Urbach tails of states coming out of both the conduction band and the valence band. The former are acceptor-like and the latter are donor-like. These tails of localized states are usually very adequately modeled by an exponential distribution increasing in concentration as the bands are approached. Of course, in crystalline materials these tails are found to fall off sharply away from the bands, whereas in amorphous materials they fall off more slowly.

The possibility of Gaussian states that are either donor-like or acceptor-like, and located anywhere in the band gap, is provided by AMPS. The possibility of a constant distribution of gap states is also included in AMPS to allow the user to introduce a background baseline of defects in a material.

These donor-like Urbach tail states coming out of the valence band are modeled in AMPS by

$$g_d(E) = G_{do}\exp(-E/E_d), \qquad (3.1.2.1.2.2a)$$

where E is measured positively up from wherever the valence band edge E_v is located at some point x. Those acceptor-like Urbach tail states coming out of the conduction band are modeled by

$$g_a(E') = G_{ao}\exp(E'/E_a), \qquad (3.1.2.1.2.2b)$$

where E' is measured negatively down from wherever the conduction band edge E_c is located at some point x. E_d and E_a are the characteristic energies that determine the slopes of their respective tails. They must be specified by the user, as must the prefactors Gdo and Gao (states per volume per energy) in these equations. Since these states can exchange carriers with the conduction and valence bands, capture-cross sections for each tail must be specified for electron capture and for hole capture These Urbach tails are seen in Fig. 3-2.

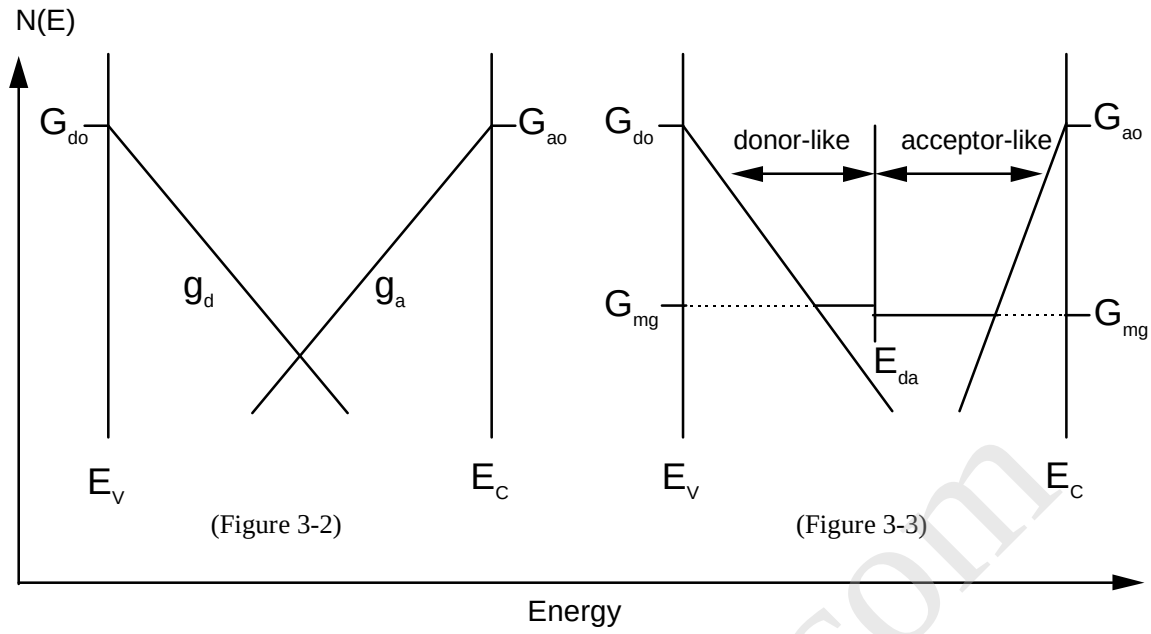

(Figure 3-2) (Figure 3-3)

Figure 3-2. Urbach tails only.

Figure 3-3. A more complicated density of states: Urbach tails and a constant mid-gap distribution (contributions from constant distribution are ignored beyond E_{Lo} and E_{Up}.

The Gaussian distributions provided by AMPS are of the form

$$g_{a,d}(E) = G_{Gd,a} \exp\left\{-\frac{1}{2}\left[\frac{\left(E-E_{pkd,a}\right)^2}{\sigma_{d,a}^2}\right]\right\} \qquad (3.1.2.1.2.2c)$$

where the prefactor G_{Gd} (for donors) or G_{Ga} (for acceptors) is in states per volume per energy. Here E_{pkd} locates the center of a donor Gaussian with respect to the conduction band and E_{pka} locates the center of an acceptor Gaussian with respect to the valence band. The quantity $\sigma_{d,a}$ is the standard deviation.

Rather than requiring $G_{Gd,a}$, AMPS is set-up to ask for the total number of states per volume in a Gaussian. It also needs $E_{pkd,a}$, $\sigma_{d,a}$, and a set of capture cross-sections for each Gaussians. All of these quantities must be inputted by the user into AMPS as is needed to describe the situation to be analyzed by AMPS.

The constant density of states distribution also provided by AMPS can be donor-like from the valence band edge E_v up to an energy E_{da} specified by the user. From E_{da} to the conduction band E_c, these states can be acceptor-like. The value of the constant density of states E_{MGD} (states per volume per energy) below E_{da} need not be the same as the value of the constant density of states G_{MGA}(states per volume per energy) above E_{da}. This "switch-over" energy E_{da} is measured positively up from E_v in AMPS. Both the constant acceptor and constant donor distributions must each be assigned a set of capture cross-sections.

AMPS computes the populations of the Urbach tail states, Gaussians, and any constant density of states distributions using Equations 2.1.2.2c and d, developed in Chapter 2. The occupation functions in these expressions are given by Equations 2.1.2.1u and v. The n and p appearing in Equations 2.1.2.1u and v are given by Equations 3.1.2.1.1a and 3.1.2.1.1c, respectively, for our single crystal layer of Fig 3-1. These expressions are all valid for both biasing situations (voltage, light, or both) and thermodynamic equilibrium. In the latter case, AMPS uses the thermodynamic equilibrium values of n and p in Equations 2.1.2.1u and v. AMPS computes the recombination traffic through exponential tail, Gaussian, and any constant density of states distribution by using the seventh and eighth terms of Equation 2.2.2.2a.

To reiterate we see from our description of these continuous state distributions and from our outline of the computations involved in determining their contributions to n_t, p_t, and recombination that the user must input the appropriate material parameters when these states are present. For the donor Urbach tails, the user must input G_{do} and E_d as well as the capture cross-sections. For the acceptor Urbach tail the corresponding quantities are required. For the Gaussian donor or acceptor distributions the densities of states in the Gaussians, peak energy, standard deviation, and capture cross-sections must be input by the user if they are needed in modeling. For the constant distributions, G_{MGA}, G_{MGD}, and E_{da} are required as are the capture cross-sections. AMPS allows the capture cross-sections to be different for the acceptor and donor states of this type.

3.1.2.1.3 Parameters for Optical Properties

The optical properties of the region seen in Figure 3.1 are specified by absorption coefficients and by relative dielectric constants. The absorption coefficients for this material are entered in tabular form as a function of wavelength.

3.1.2.2 Parameters for Amorphous Semiconductor Materials

In this section, we now consider the layer of semiconductor material seen in Fig. 3-1. to be an arbitrary amorphous semiconductor with constant material properties. We do not specify where it is in the device; it simply is an amorphous semiconductor layer existing somewhere in a device. We also note that all of the delocalized state, gap state, and optical parameters described in section 3.1.2.1 are applicable to this amorphous layer. The major difference between amorphous and single crystal semiconductors is the low mobility and the large numbers of localized gap states in amorphous semiconductors. The user simply reflects the enhanced role of gap states in amorphous materials by appropriate adjusting the input parameter values for the various gap state models discussed in Section 3.1.2.1.

Also, it may be necessary when modeling amorphous materials to differentiate between a mobility gap E_{Gu} and an optical gap $E_{Gop.}$ In single crystal materials $E_{Gu}=E_{Gop}=E_G$; however, in amorphous materials the states that support delocalized band transport may exist at a different threshold from those states that support band-to-band optical transitions. In AMPS $E_{Gu}=E_c-E_v$ and E_{Gop} may be separately inputted by the user. We note that AMPS measures all energies defining gap state distributions in terms of E_{Gu}; that is, from E_v or E_c as discussed in Section 3.1.2.1.

We also note that E_{gop} is only present in AMPS for book-keeping, that is, what really determines what wavelengths cause photogenerated carriers is the absorption coefficient table. If there is an absorption coefficient present for some wavelength, then AMPS assumes the absorption produced

photocarriers in the bands. Hence E_{gop} and the absorption table should be self-consistent but it really is the absorption table tat controls the threshold of photocarrrier generation.

We stress here that by combining the exponential, Gaussian, rectangular, and discrete energy distributions discussed in Section 3.1.2.1 and available in AMPS, any density of states profile in an amorphous material can be simulated. For example the Urbach tails which are so important in amorphous semiconductors are modeled by the exponential distributions built into AMPS. The dangling bonds of a-Si:H are, for example, also easily modeled by AMPS using the Gaussian distributions that are also built in.

3.1.2.3 Parameters for Polycrystalline Semiconductor Materials

In this section we now address the possibility that all of, or some part of, a device structure may be composed of polycrystalline semiconductor material. Polycrystalline semiconductors are materials that have crystalline regions (grains) which are bounded by disordered regions (grain boundaries). To simulate polycrystalline materials with AMPS, one need only to create a multi-region structure consisting of crystalline regions interspersed with thin amorphous regions. The crystalline regions represent the semiconductor grains, while the thin amorphous regions represent the disordered grain boundaries. With this approach of allowing for regions of different material parameters, AMPS can simulate an extremely general semiconductor device structure that can consist of any combination of single crystal, polycrystalline, and amorphous semiconductors.

3.2 Parameters for Insulator Properties

Insulators can be modeled using AMPS by assuming a wide bandgap material. This can easily be done by making E_G large. If the insulator is ideal, one can choose E_G to give a desired conductivity (or resistivity) by the formula $\sigma = q(\mu_n+\mu_p)n_i = q(\mu_n+\mu_p)\sqrt{N_cN_v}\exp(-E_G/kT)$.. Of course, all of the material parameters discussed in Section 3.1.1. are available for this insulating material. Consequently, deviations from the "perfect" insulator can be modeled by inputting gap states that can, of course, have properties that vary with energy and position.

3.3 Parameters for Metal Properties

In AMPS, metals may exist at the contacts at x=0 and x=L. The general boundary conditions used by AMPS allow for modeling of a wide variety of these metal contacts. In AMPS one inputs the appropriate barrier height and electron affinity at the front (x=0) and back (x=L) of the device structure, thereby establishing the work function of the metal from

$$\phi w,front = \phi bo + \chi(x=0) \tag{3.3a}$$

$$\phi_{w,back} = \phi_{bL} + \chi_{(x=L)} \tag{3.3b}$$

By choosing barrier heights (i.e., the metals) and surface recombination speeds (the quality of interface) one can enhance or reduce the quality of the semiconductor contact and, hence, ideal ohmic, non-ideal ohmic or rectifying contacts can be modeled. For example, a low barrier contact with high surface recombination speeds could represent an ideal metal contact, while the same

contact with low surface recombination speeds could represent a poorly prepared surface or an electrolytic contact.

We note that AMPS also allows for tunneling at contacts; however this feature is currently not in AMPS-1D.

3.4 Parameters for Interface Properties

The contacts at x=0 and x=L caused by the presence of metals can be thought of as special interfaces. From Section 3.3 it follows that these contacts are fully specified by inputting the barrier height and the surface recombination speeds for each carrier. As was discussed in Section 2.2.4, AMPS allows for transport at these contacts from recombination to thermionic emission to be rigorously modeled, as outlined in Section 2.2.4; by adjusting the effective surface recombination speeds. If tunneling is chosen to be present by the user, it exists parallel to the other transport mechanisms at the contact. Invoking the presence of direct tunneling for a carrier necessitates that the user input an effective tunneling mass for the carrier. Again tunneling is not currently available in AMPS-1D.

These special interfaces at x=0 and x=L which are the metal contacts also have optical properties. These are captured in reflection coefficients R_F and R_B.

AMPS allows interface regions to be created adjacent to these contacts as x=0 and x=L and to be created anywhere in a device. These interface regions are thin regions which have a large number of defect states. The user can input an interfacial layer anywhere by adding a thin region with different properties. Often people speak in terms of the interfacial area defect density at an interface. This can be computed by multiplying the volume density of states in the interfacial layer by the thickness of the interfacial region. We stress that, since this interfacial region can have its own material parameters, the user can create an interfacial layer that is entirely independent of the surrounding bulk materials.

3.5 Parameters for Materials with Spatially Varying Properties

The discussions in the previous sections have pointed out the great range of the material parameters and device structures that AMPS can simulate. In particular, as has been mentioned in the discussions on polycrystalline grain boundaries and interfaces, AMPS can model structures with as many different regions of different material parameters as desired. By judiciously positioning these different material layers, regions of continuously-varying material parameters can be created. This ability to spatially vary material parameters gives the user a great deal of flexibility in creating a very general device structure using AMPS. Chapter 4 detail the input parameters.

CHAPTER 4
PROCEDURE FOR RUNNING AMPS

4. 1 Overview

First AMPS will calculate the basic band diagram, built-in potential, electric field, free carrier populations, and trapped carrier populations present in a device when there is no (voltage or light) biasing of any kind. These thermodynamic equilibrium solutions allow the device designer to "see what the device will look like."

Then AMPS will take these thermodynamic equilibrium solutions and use them as starting guesses for the iterative scheme that will lead to the complete characterization of a device under voltage bias, illumination bias, or voltage and illumination bias. AMPS will generate output such as the band diagram (including quasi-Fermi levels), carrier populations, currents, recombination profiles, current-voltage (I-V) characteristics, and spectral response can be obtained for devices under various levels of voltage, illumination, or voltage and illumination bias.

4. 2 How to Generate Device Characteristics

4. 2. 1 Dark IV Characteristics

In the window where user specify the voltage bias conditions, all you have to do is give the range of voltage biasing. For example, voltage biasing from -1v to 1v. This voltage range will apply not only to dark I-V, but also light I-V. If user want to see band diagram at certain bias condition, he (she) may open the window of selected biasing to give AMPS the value Thai must: 1) fall into the voltage he (she) specified in the previous window; 2) be consistent with voltage step chosen before. For example, if a user choose a voltage step as 0.05 volts between 0 and 1 volts and he wants to see the band diagram at 0.88 volts. AMPS will round it off to 0.9 volts. In this case user has to reduce his voltage step to 0.04 volts at least. Note that the more voltage points you input, the longer time AMPS will take to calculate.

4. 2. 2 Light IV Characteristics

The only difference between light and dark IV at user input window is that user has to check "light on " at the illumination window. AMPS provided AM1.5 as default, but the photon flux and spectrum can be defined by user. A neutral filter/concentrator is given as a box named "light-x". The absorption coefficient has to be input by user manually. But AMPS does provide a option in the box "Eopt" for user to linearly shift the absorption coefficient. Because most of the time the data of absorption coefficient is not easy to obtain, this linear shift may help user to count the change of band gap. Details can be seen at user interface.

4. 2. 3 Spectral Response

If user want to see the current generated at each wavelength, he (she) has to check "spectral response" box. AMPS will always generate spectral response both with and without light bias. The light bias is defined by the spectrum and flux in the spectrum window. The range of QE plot is also determined by this spectrum defined by user. User can change the probe beam intensity as well. AMPS can generate QE at specified voltage bias as long as the voltage point obey the rules described above.

4. 3 Surface Photovoltage Response

Typically, the SPV technique is performed using one of two methods: Method A or Method B. [1,2] Basically, both methods involve a relationship between four quantities: the open circuit voltage Voc, the photon flux intensity Φo, the light penetration depth $1/\alpha$ at known wavelengths λ of monochromatic light, and the minority carrier diffusion length Ln (p-type). Both methods require a linear relation between the independent variable (which differs for Methods A and B) and the dependent variable $1/\alpha$ (which is the same for both methods). With Method A, if Voc is held constant while λ is varied, then the required linear relationship must be formed in a plot of Φo versus $1/\alpha$. This plot, when extrapolated to the $1/\alpha$ axis, yields Ln, according to Method A. With Method B, on the other hand, if Φo is held constant while λ is varied, then the required linear relationship must be found in a plot of 1/Voc versus $1/\alpha$. This plot, when extrapolated to the $1/\alpha$ axis, yields the correct value of Ln according to Method B.

1. A.M. Goodman, "A Method fro the Measurement of short Minority Carrier Diffusion Lengths in Semiconductors," Journal of Applied Physics, 32 (1961) P.2550

2 A. Quilliet and M.P. Gosar, "L'Effet Photovoltaique De Surface Dans Le Silicium Et Son Application A La Mesure De La Duree De Vie Des Porteurs Minoritaires," Journal de Physique et le Radium, 21 (1960), pp 3335-3338

4.4 Procedure for Inputting Parameters

When you run one of our simulations, the program expects a default set of parameters. We have created a default set of parameters for a-Si:H and for a crystalline silicon p-n junction that can always be used. Our intent is that most people will start with the our default files and modify them as appropriate crating their own default cases. If you have an old case saved in one of your directories and you would like to use these parameters as your default file, you can do so by **saving the old case as the case name you wish and reset the parameters**. This default option can be useful if you have previously run a case similar to your current interests, and you wish only to change a few parameters.

Once the program has accepted the default parameters, you may edit them as desired to fit your particular configuration. You may review all of the parameters by selecting the appropriate options when they are displayed on the screen.

4.4.1 List of Input Parameters

The following is a list of input parameters that AMPS needs to solve the set of transport equations and boundary conditions. In general, this list will apply to all current program versions, with some minor exceptions. The differences in the parameter list between each program version will be mentioned as they are discussed. Parameters which only apply to non-equilibrium are tagged.

For the programs of all parameters fall into one of three general categories:

1. Parameters that apply over the entire device.
2. Parameters that apply to a particular region.
3. Parameters that define the illuminating spectrum (for cases with light).

4.4.1.1 Parameters that Apply to the Entire Device

The parameters that apply to the entire device (category 1) include (units used in AMPS are in parentheses) the following:

1. Boundary conditions

   Please see Figure 4-1 for more details on where PSIBO and PSIBL are applied.

   a. PHIBO = $\Phi_{b0} = E_C - E_F$ at x=0 (eV)

   b. PHIBL = $\Phi_{bL} = E_C - E_F$ at x=L (eV)

2. Surface recombination speeds[4,5]

   a. SNO = S_{NO} = electrons at x=0 interface (cm/sec)

   b. SPO = S_{PO} = holes at x=0 interface(cm/sec)

   c. SNL = S_{NL} = electrons at x=L interface (cm/sec)

   d. SPL = S_{PL} = holes at x=L interface (cm/sec)

3. Reflection coefficient for light impinging on front and back surfaces

   a. RF = R_F = reflection coefficient at x=0 (front-surface)

   b. RB = R_B = reflection coefficient at x=L (back-surface reflection)

4. Temperature T (K)

These parameters are entered only once, and apply in general to the entire device.

[4] These parameters are unique to non-equilibrium.

[5] By taking S=1/4(thermal velocity), AMPS will then be modeling thermionic emission for that carrier and plane.

4.4.1.2 Parameters that Apply to a Particular Region

The parameters in Category 2, however, may have different values in different regions. These parameters include (units in parentheses):

1. The width W or XLAYER (A) of a region
2. Basic material properties

   Figure 4-1 shows a band diagram with CHI, EG, etc.

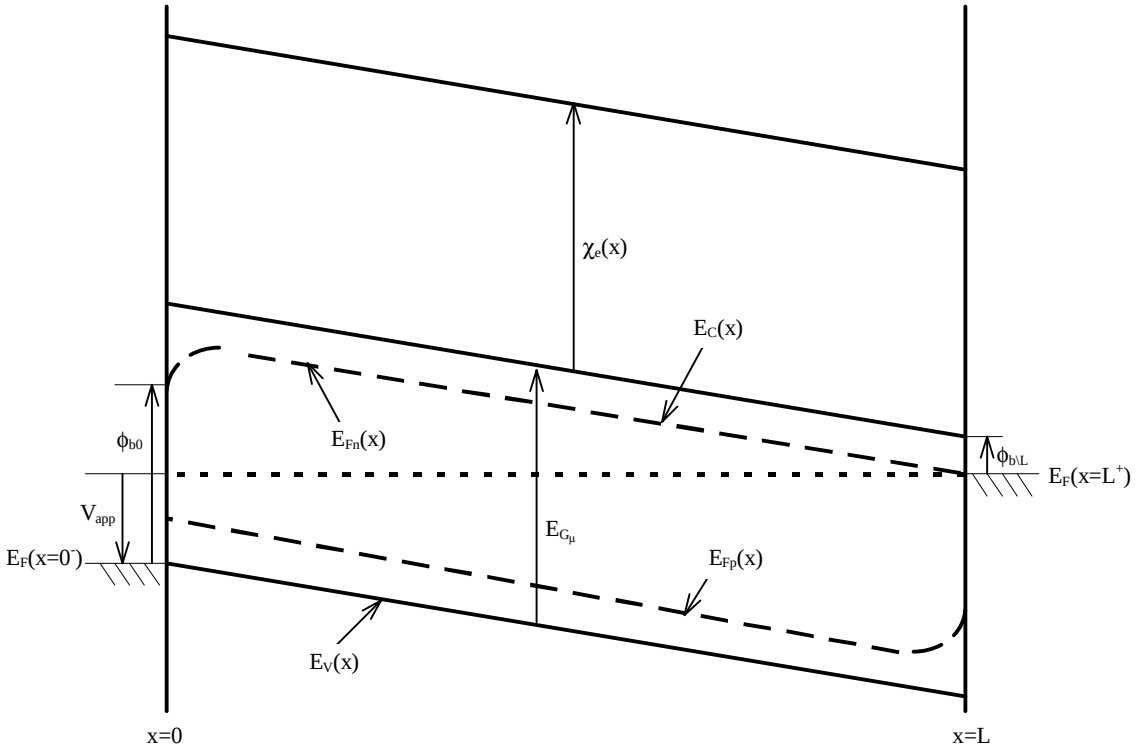

Figure 4-1 Schematic band diagram of a semiconductor device under an applied voltage V_{app} .

a. EPS = relative permittivity ε_r at temperature T such that $\varepsilon_s = \varepsilon_r\varepsilon_0$, where ε_s is the permittivity of the semiconductor.

b. NC = effective density of states N_C (cm^{-3}) in the conduction band at temperature T

c. NV = effective density of states N_V (cm^{-3}) in the valence band at temperature T

d. EG = the mobility bandgap $E_{G\mu}$ (eV) at temperature T

e. EGOP = the optical bandgap E_{Gopt} (eV) at temperature T

> **NOTE**: This parameter determines the longest wavelength photon used in calculating photo generation. Even if absorption coefficients are entered for $\lambda > E_{gopt}/1.24$, these wavelength will not be used for calculations such as those needed for J_{sc} and QE.

f. CHI = electron affinity χ_e (eV) at temperature T

g. MUN[4] = Electron mobility μ_n (cm^2/V-sec) at temperature T

h. MUP[4] = Hole mobility μ_p (cm^2/V-sec) at temperature T

3. Discrete Localized Defect States

DLVS is the number of discrete donor-like levels (0≤DLVS≤25) and ALVS is the number of discrete acceptor-like levels (0≤ALVS≤25). Figure 4-2 shows the variables EDON, EACP, ND, NA, WDSD, and WDSA.

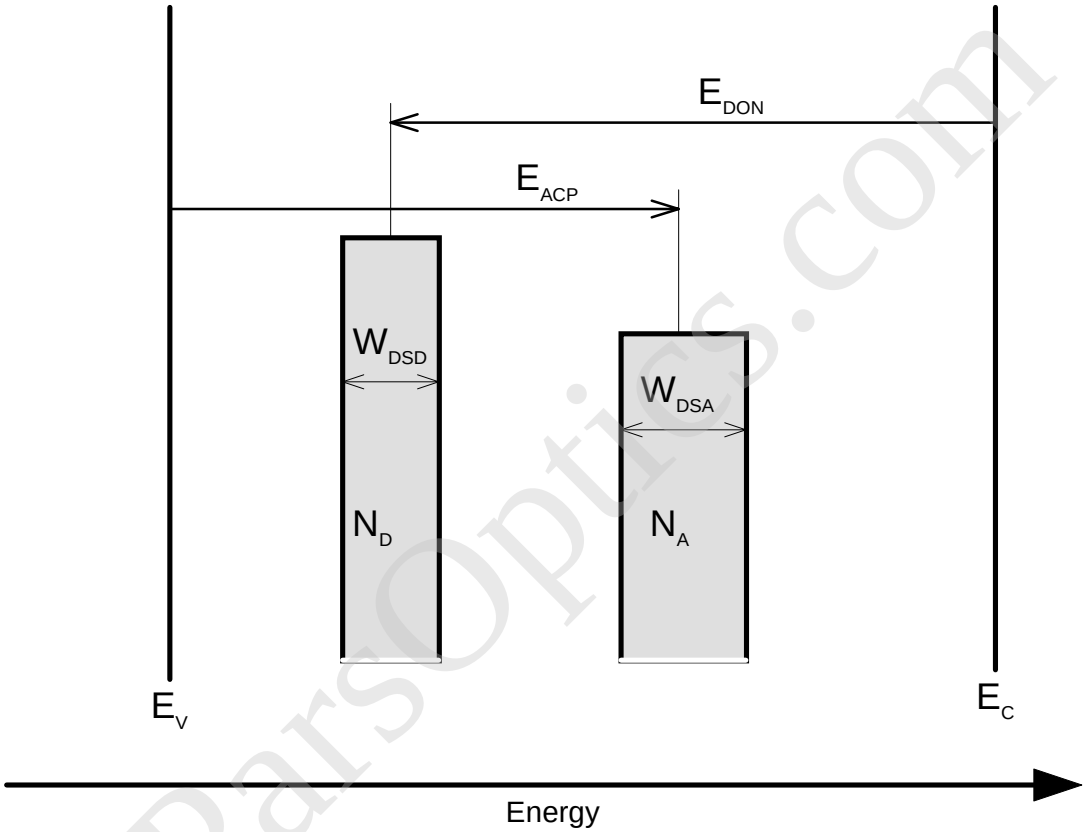

Figure 4-2 An example of one discrete donor level and one discrete acceptor level.

a. Discrete donor level concentrations and ionization energies

i. For full ionization input DLVS = 0 and the following

a) ND(i) = $N_{D,i}$ = Concentration (cm^{-3}) at the i^{th} donor level

ii. If DLVS>0 (partial ionization), then input for each of the i = DLVS discrete levels

a) ND(i) = $N_{D,i}$ = Concentration (cm^{-3}) at the i^{th} donor level

b) EDON(i) = Ionization energy (eV) of the i^{th} donor level measured positively from the conduction band edge E_C

c) WDSD(i) = $W_{D,i}$ = Width (eV) of the i^{th} banded donor dopant level

d) DSIG/ND(i)[4] = Electron capture cross section. (cm^2) for the ith discrete donor level

e) DSIG/PD(i)[4] = Hole capture cross section (cm^2) for the ith discrete donor level

b. Acceptor level concentrations and ionization energies

i. For full ionization input DLVS = 0 and the following

a) NA(i) = $N_{A,i}$ = Concentration (cm^{-3}) at the ith acceptor level

ii. If ALVS>0 (partial ionization), then input for i=1 to ALVS,

a) NA(i) = $N_{A,i}$ = Concentration (cm^{-3}) at the ith acceptor level

b) EACP(i) = Ionization energy (eV) of the ith acceptor level measured positively from the valence band edge E_V

c) WDSA(i) = $W_{A,i}$ = Width (eV) of the ith banded acceptor dopant level

d) DSIG/NA(i)[4] = Electron capture cross section (cm^2) for the ith discrete acceptor level

e) DSIG/PA(i)[4] = Hole capture cross section (cm^2) for the ith discrete acceptor level

4. Continuous Localized Defects in the Tails and Midgap States (SHAPE = "V" or "U")

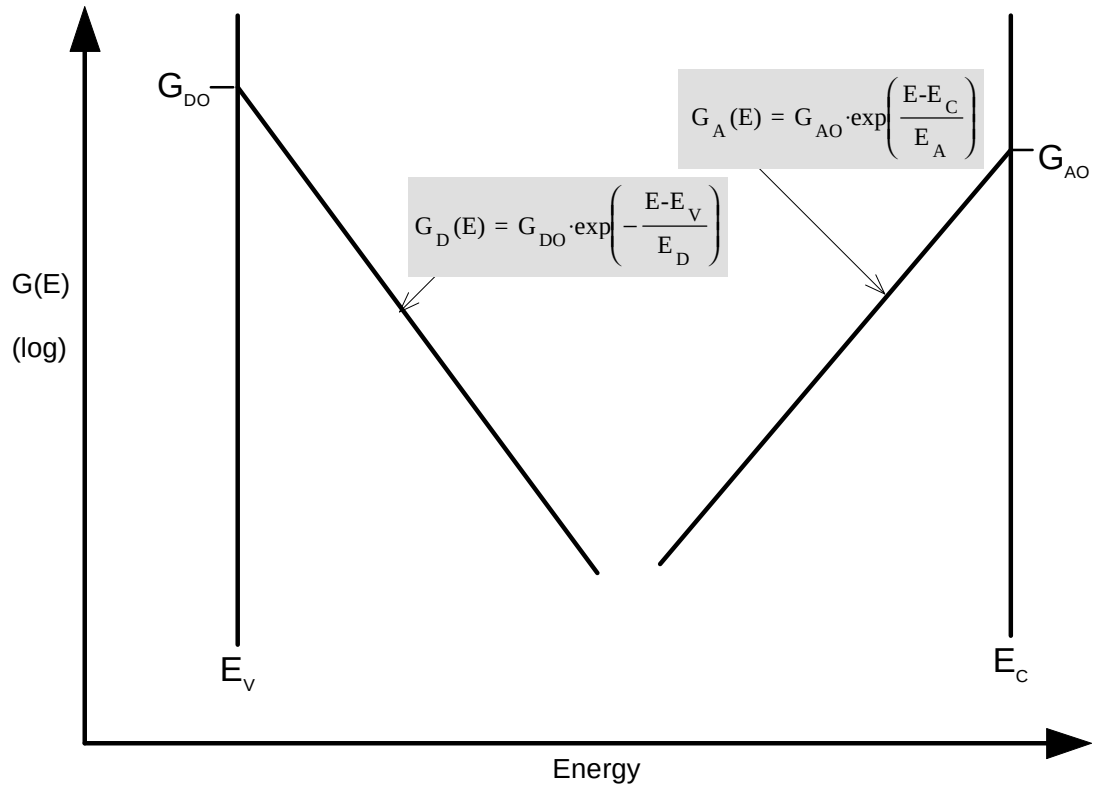

Figure 4-3 "V-shaped" representation of density of states.

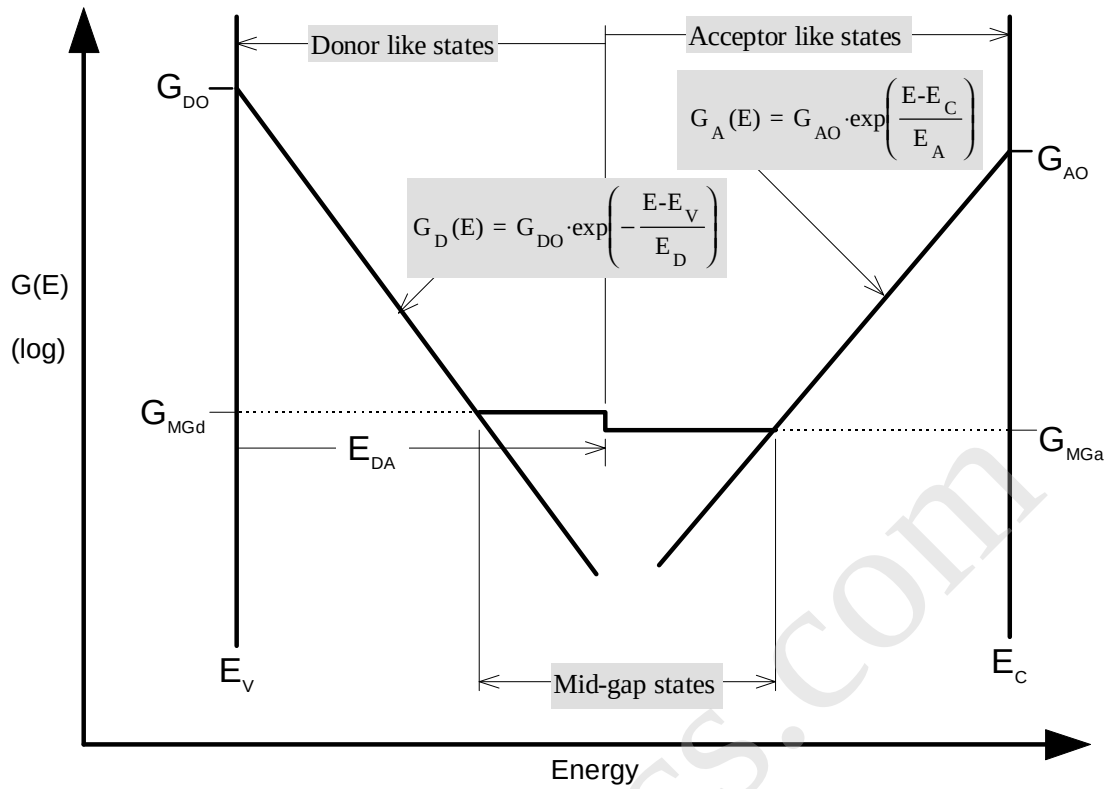

Figure 4-4. "U-shaped" representation of the density of states.

a. If "V-shaped", then the following apply

   i. GDO = Prefactor (in $1/cm^3/eV$) in equation: $gd= G_{do}exp(E-E_V/E_d)$
   ii. GAO = Prefactor (in $1/cm^3/eV$) in equation: $ga= G_{ao}exp(E-E_C/E_a)$;
   iii. ED = Characteristic energy E_d (eV) for donor-like tails
   iv. EA = Characteristic energy E_a (eV) for acceptor-like tails
   v. TSIG/ND[4] = Capture cross section for electrons in donor tail states (cm^2)
   vi. TSIG/PD[4] = Capture cross section for holes in donor tail states(cm^2)
   vii. TSIG/NA[4] = Capture cross section for electrons in acceptor tail states (cm^2)
   viii. TSIG/PA[4] = Capture cross section for holes in acceptor tail states (cm^2)

b. If "U-shaped" then the following apply *in addition to the "V-shaped" parameters*

   i. GMGA = Density of midgap acceptor-like states G_{MGa} ($1/cm^3/eV$)
   ii. GMGD = Density of midgap donor-like states G_{MGd} ($1/cm^3/eV$)
   iii. EDA = "Switch-over energy" E_{DA} (eV) measured positively from E_V
   iv. MSIG/ND[4] = Capture cross section for electrons in donor midgap states (cm^2)
   v. MSIG/PD[4] = Capture cross section for holes in donor midgap states(cm^2)
   vi. MSIG/NA[4] = Capture cross section for electrons in acceptor. midgap states (cm^2)
   vii. MSIG/PA[4] = Capture cross section for holes in acceptor midgap states (cm^2)

5. Gaussian levels (0, 1, or 2 acceptor and 0, 1, or 2 donor levels)

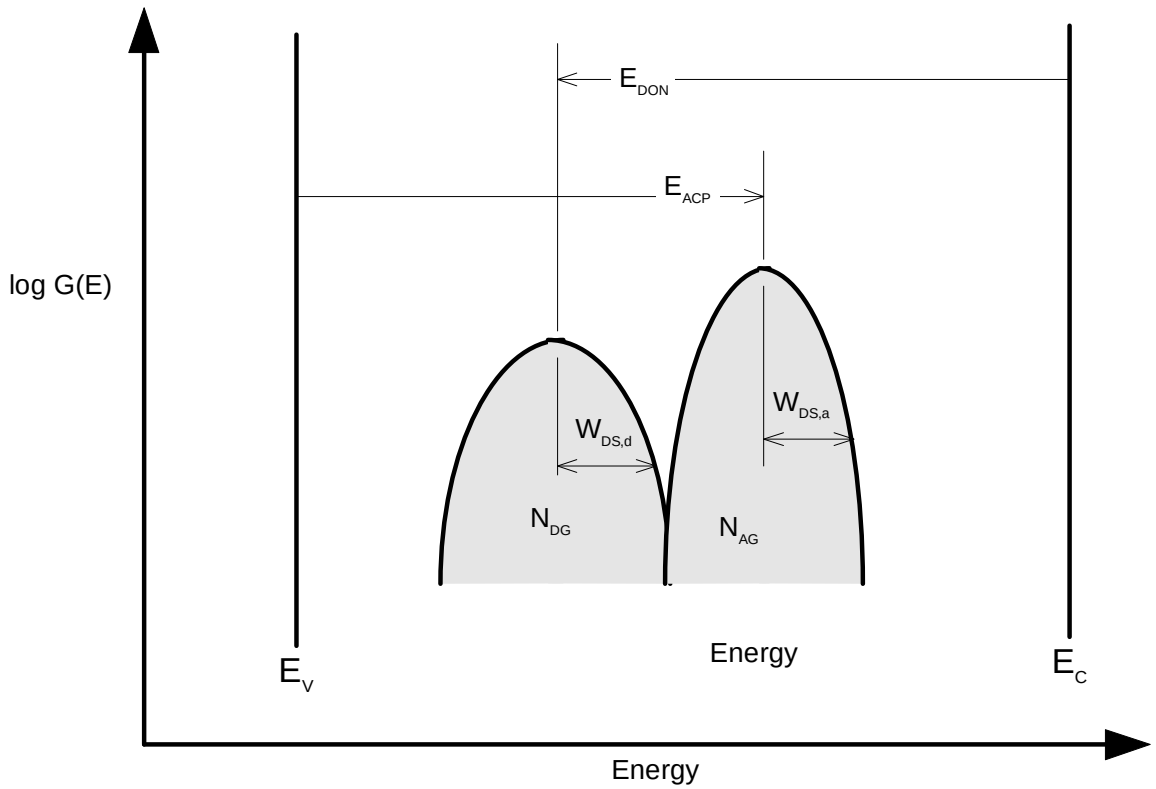

Figure 4-5 An example of one Gaussian donor level and one Gaussian acceptor level.

a. Number of Gaussian donor levels. If DLVSG > 0, then enter the following which are referenced in Figure 4-5 for each of the i = DLVSG ≤ 2 Gaussian donor levels.

   i. NDG(i) = The Gaussian donor state density ($1/cm^3$) for the i^{th} donor Gaussian

   ii. EDONG(i) = The donor Gaussian peak energy (eV) measured positive from E_C for the i^{th} donor Gaussian

   iii. WDSDG(i) = The standard deviation (eV) of the i^{th} Gaussian donor level

   iv. GSIG/ND(i)[4] = Capture cross section of the i^{th} donor-like Gaussian state for electrons (cm^2)

   v. GSIG/PD(i)[4] = Capture cross section of the i^{th} donor-like Gaussian state for holes (cm^2)

b. Number of Gaussian acceptor levels. If ALVSG > 0, then enter the following which are referenced in Figure 4-5 for each of the i = DLVSG ≤ 2 Gaussian acceptor levels.

   i. NAG(i) = The Gaussian acceptor state density ($1/cm^3$) for the i^{th} acceptor Gaussian

   ii. EACPG(i) = The acceptor Gaussian peak energy (eV) measured positive from E_V for the i^{th} acceptor Gaussian

   iii. WDSAG(i) = Standard deviation (eV) of the i^{th} Gaussian acceptor level

   iv. GSIG/NA(I)[4] = Capture cross section of the i^{th} acceptor-like Gaussian state for electrons (cm^2)

v. GSIG/PA(I)[4] = Capture cross section of the i^{th} acceptor-like Gaussian state for holes (cm^2)

4.4.1.3 Parameters that Define the Illumination Spectrum

The third set of parameters are those used to define any impinging illuminated spectrum as well as the absorption coefficients. These parameters are obviously necessary if the device is under illumination. The first of these parameters, called LIGHT in our program, determines if light is desired in the program. If LIGHT = NO, then no spectrum need to be defined and the user is only interested in the device characteristics in the dark under voltage bias. If, however, the user wishes to have the device under illumination, then for each wavelength in the spectrum, the following parameters need to be defined (units in parentheses):

1. The wavelength LAMBDA (μm)
2. The incident FLUX at this wavelength ($1/cm^2/sec$)
3. The absorption coefficient ALPHA (1/cm) at that wavelength in each region of the structure. We emphasize that this information must be specified by the user for each region of the device structure.

In addition, the user has the option of calculating the quantum efficiency, (also called spectral response or SR) which is current per unit flux for each band width. This SR may be calculated at short circuit (which is the usual experimental situation) or at various forward and reverse bias situations. If a spectral response (SR) is requested, then the flux level (SRFLUX) of the probing stepped monochromatic light used in such a measurement must be specified. This freedom is provided, since, in general, the spectral response may be different for different values of flux. If light bias is chosen, the spectrum of that bias light, present while the superimposed monochromatic radiation is varied throughout the response range, is chosen by the user.

4.5 Choosing A Grid

To obtain valid results from AMPS good grid spacing must be chosen. AMPS offers both equal grid spacing and variable grid spacing. All program versions offer equal grid spacing and some offer variable grid spacing. If you use equal grid spacing, AMPS will always use 400 equally spaced points. The number 400 is an arbitrarily chosen upper bound we are now using for the total number of points Most of the time 400 equally spaced points are adequate for AMPS to quickly find valid results. However, if the simulation is rather complex or better performance is wanted, use variable grid spacing. This gives the user the ability to adjust both the number of points and their location. (To use variable grid spacing append a "v" to the end of the program version name.) An optimized grid allows AMPS to quickly calculate valid results. AMPS can do this if the grid provides the minimum number of grid points clustered in regions where the fields and material parameters are changing the most.

In AMPS is changing from the interface of each layer. The grid space at the interface of all the layers is kept same, but this value can be modified by user. AMPS allow user to specify the unique grid space in the middle of each layer. For example, if the layer is thick, user may choose a large number of grid spacing. The middle grid spacing can be any number as long as the total number

grid points has to be less than the limitation. AMPS will list the first three layers that has the most grid points and user can adjust by himself to reduce the total number.

APPENDIX A
OPTICAL GENERATION RATE

We embark on a very general derivation of the $\Phi_i^{FOR}(\nu_i)$ and $\Phi_i^{REV}(\nu_i)$ appearing in Section 2.2.3 by considering a structure with N different semiconductor regions each of thickness l_j (see Fig. A1), such that

$$\sum_{j=1}^{N} l_j = L \qquad (A.1)$$

where L is the total device length. These N regions have different physical properties. In particular, they can have different properties such as absorption coefficients; we assume that the material parameters vary from region to region but are constant within a particular region.

Since the permittivity can vary from region to region, there can be internal reflection at the boundaries of these N layers. AMPS is formulated to consider this general possibility.

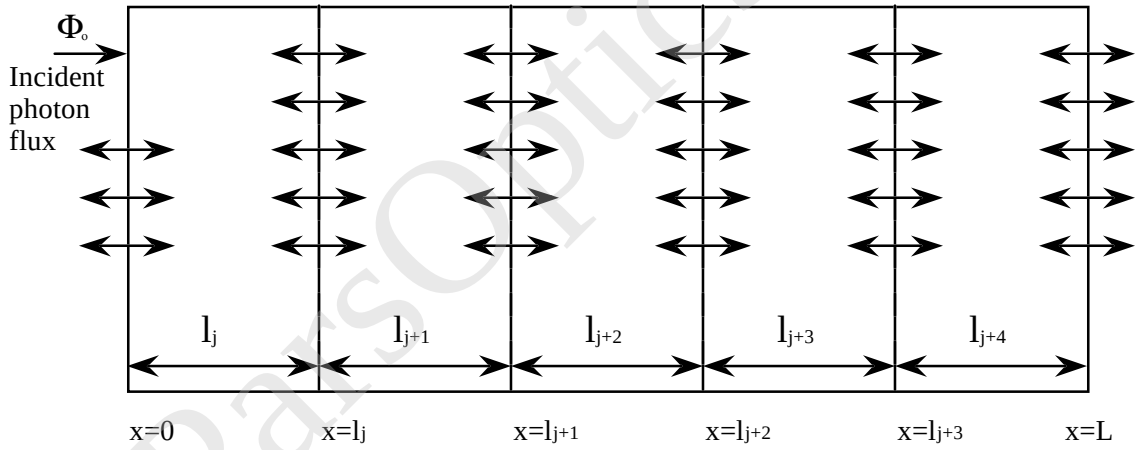

Figure A-1. Reflection and transmission within a device of five regions of differing material parameters.

To outline this formulation, we begin by assuming that the semiconductor is subject to an external source of illumination with a photon flux of Φ_{o_i} (in units of photons per unit area per unit time) impinging on $x=o^-$ (from left to right). These photons have the frequency ν_i. If $h\nu_i$ is greater than $E_{g_{op}}$ somewhere in the device (the optical bandgap), then optical generation takes place and a free electron-hole pair is produced. The flux transmitted through the back contact Φ_L^{RL} into the material at $x=L^-$ is zero since AMPS assumes that no illumination is impinging from the back; i.e.,

$$\Phi_L^{RL} = 0 \qquad (A.3)$$

The flux $\Phi_i(x)$ set-up in the j+1 material layer by this illumination of frequency ν_i, allowing for multiple reflections at the j and j+1 boundaries of this layer, is

$$\Phi_i(x) = \Phi_j^{LR} e^{-\alpha_{j+1}(x-x_j)} + \Phi_{j+1}^{RL} e^{-\alpha_{j+1}(x_{j+1}-x)}$$
$$+ R_j \Phi_{j+1}^{RL} e^{-\alpha_{j+1} l_{j+1}} e^{-\alpha_{j+1}(x-x_j)} + R_{j+1} \Phi_j^{LR} e^{-\alpha_{j+1} l_{j+1}} e^{-\alpha_{j+1}(x_{j+1}-x)}$$
$$+ R_j R_{j+1} \Phi_j^{LR} (e^{-\alpha_{j+1} l_{j+1}})^2 e^{-\alpha_{j+1}(x-x_j)} + R_{j+1} R_j \Phi_{j+1}^{RL} (e^{-\alpha_{j+1} l_{j+1}})^2 e^{-\alpha_{j+1}(x_{j+1}-x)}$$
$$+ R_j R_{j+1} R_j \Phi_{j+1}^{RL} (e^{-\alpha_{j+1} l_{j+1}})^3 e^{-\alpha_{j+1}(x-x_j)}$$
$$+ R_{j+1} R_j R_{j+1} \Phi_j^{LR} (e^{-\alpha_{j+1} l_{j+1}})^3 e^{-\alpha_{j+1}(x_{j+1}-x)} + \ldots + \ldots \qquad (A.4)$$

This expression arises by assuming some flux Φ_j^{LR} enters the j+1 material layer at x_j and some flux Φ_{j+1}^{LR} enters this material layer at x_{j+1} due to reflection at the back contact and at material interfaces to the right of $x=x_{j+1}$. Equation A.4 then follows by computing the multiple reflections that these two fluxes undergo inside this j+1 material.

If there are N different material regions, then there are N-1 Φ^{LR} and N-1 Φ^{RL} values in Equation A.4 to be determined for each frequency ν_i. Once these are determined, then $\Phi_i(x)$ is completely known and the $\Phi_i^{FOR}(\nu_i)$ of Equation 2.2.3f and the $\Phi_i^{REV}(\nu_i)$ of Equation 2.2.3g are also known for the j+1 material. The latter statement follows from the fact that the odd numbered terms of the right-hand side of Equation A.4 can be seen to be $\Phi_i^{FOR}(\nu_i)$, whereas the even numbered terms can be seen to be $\Phi_i^{REV}(\nu_i)$.

The determination of the Φ^{RL} for the j^{th} material layer can be achieved by recognizing that Φ^{RL} at the j^{th} boundary must be equal to the function $\Phi^{REV}(\nu_i)$, present in the $(j+1)^{th}$ layer, evaluated at $x=x_j$ and multiplied by $(1-R_j)$, viz.,

$$\Phi_j^{RL} = (1-R_j)\{\Phi_{j+1}^{RL}[(e^{-\alpha_{j+1} l_{j+1}}) + R_{j+1} R_j (e^{-\alpha_{j+1} l_{j+1}})^3 + \ldots]$$
$$+ R_{j+1} \Phi_j^{LR}[(e^{-\alpha_{j+1} l_{j+1}})^2 + R_{j+1} R_j (e^{-\alpha_{j+1} l_{j+1}})^4 + \ldots]\} \qquad (A.5)$$

Similarly, Φ^{LR} at the $(j+1)^{th}$ boundary must be $\Phi^{FOR}(\nu_i)$ for the $(j+2)^{th}$ evaluated at $x=x_{j+1}$ and multiplied by $(1-R_{j+1})$. The result is

$$\Phi_{j+1}^{LR} = (1-R_{j+1})\{\Phi_j^{LR}[(e^{-\alpha_{j+1} l_{j+1}}) + R_{j+1} R_j (e^{-\alpha_{j+1} l_{j+1}})^3 + \ldots]$$
$$+ R_j \Phi_{j+1}^{RL}[(e^{-\alpha_{j+1} l_{j+1}})^2 + R_{j+1} R_j (e^{-\alpha_{j+1} l_{j+1}})^4 + \ldots]\} \qquad (A.6)$$

The needed 2(N-1) values of Φ^{LR} and Φ^{RL} are obtained by AMPS by solving the 2(N-1) equations of the type A.5 and A.6 and by using Equation A.2 and Equation A.3. Once these are obtained for each frequency ν_i the $\Phi_i^{FOR}(\nu_i)$ and $\Phi_t^{REV}(\nu_i)$ are completely specified and, thus, $G_{op}(x)$ can be evaluated.

APPENDIX B
TRIAL FUNCTION FOR THE CURRENT DENSITY

The first term in the continuity equations (Equations 2.2a and b) is the derivative of the current densities. Typically, the current densities for holes and electrons are represented, by [2]

$$J_p = -q\mu_p p\left(\frac{dE_{f_p}}{dx}\right) \tag{B-1}$$

and

$$J_n = q\mu_n n\left(\frac{dE_{f_n}}{dx}\right) \tag{B-2}$$

The signs in Equations B-1 and 2 are chosen to be consistent with our measuring scheme for E_{f_p} and E_{f_n} (Fig. 3-2). Quasi-Fermi level formulations for J_p and J_n are used in AMPS because they allow for diffusion, for drift, and for effective forces that may arise from material property variations [1]. This quasi-Fermi level formulation is also used in AMPS because it avoids the possible problem of adding diffusion and drift currents to get the total current. This is a possible numerical problem, because both current components could be large yet their algebraic sum could be very small.

The above expressions for J_p and J_n cannot be used as they stand in the necessary numerical solution scheme of AMPS. When they are expressed as differences in representing the dJ_p/dx and dJ_n/dx terms of Equations 2.2a and b, numerical methods have extreme difficulty in converging to a solution. To avoid this well-known problem, Scharfetter and Gummel derived "trial functions" based on Equations B-1 and B-2 for the current densities which can then be used to evaluate dJ_p/dx and dJ_n/dx in an approach that is much more amenable to numerical methods [3]. The trial functions are derived here for reference.

Figure B.1 shows a device that has N slabs and N+1 major grid points. The major grid points, represented by solid lines, are the points in the device for which the unknowns, Ψ E_{f_n}, and E_{f_p} are solved. The minor grid points represented by the dashed lines, are the points in the device for which the current densities are solved in the Scharfetter-Gummel approach. To outline the Scharfetter-Gummel approach to evaluating these dJ_p/dx and dJ_n/dx terms of the continuity equation, we become specific and consider the trial function for J_p. To derive it, we begin by assuming the hole current density, described by J_p between the major grid points i and i+1, is constant and equal to $J_{p,i+1/2}$. Hence we can write

$$J_{p,i+\frac{1}{2}} = -q\mu_p p_i\left(\frac{dE_{f_p}}{dx}\right) \tag{B-3}$$

$$= -q\mu_p N_v \exp\left(\frac{\Phi_{b_L} - E_G + E_{fp} + \Psi}{kT}\right)\left(\frac{dE_{f_p}}{dx}\right) \qquad \text{(B-4)}$$

where the left hand-side of these equations are constant. The E_{F_p} and Ψ are still considered functions of x, however, multiplying both sides of Equation B-4 by $\exp(-\Psi)dx$ gives

$$J_{p,i+\frac{1}{2}} \exp(-\Psi/kT)dx = -q\mu_p N_v \exp\left(\frac{\Phi_{b_L} - E_G + E_{f_p}}{kT}\right)de_{f_p} \qquad \text{(B-5)}$$

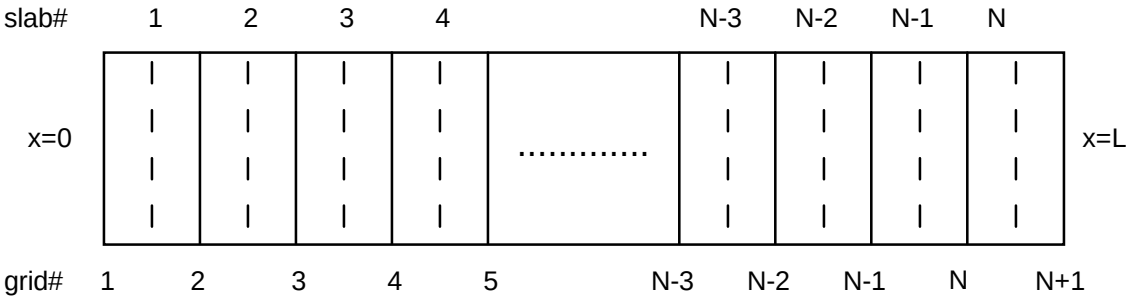

Figure B-1. A grid used in numerical methods. There are N slabs and N+1 major grid points (represented by solid lines). The dashed lines are the points where the current density trial function is solved.

It may be immediately noted that the right-hand side of B-5 can be integrated analytically. We can also analytically integrate the LHS of B-5 if we now make the additional assumption that the electric field is constant between i and i+1. Hence, we can write $\Psi(x)$ between x_i and x_{i+1}, as

$$\Psi(x) = \left[\frac{\Psi_{i+1} - \Psi_i}{H}\right](x - x_i) + \Psi_i$$

where H is the forward difference between adjacent grid points. This expression, which when substituted into B-5, allows the LHS to integrate to

$$J_{p,i+\frac{1}{2}} \cdot \left[kT \cdot \frac{\exp(-\Psi_{i+1}/kT) - \exp(-\Psi_i/kT)}{(\Psi_{i+1} - \Psi_i)/H}\right] \qquad \text{(B-6)}$$

while integrating the right-hand side of Equation B-5 gives

$$\int_i^{i+1} q\mu_p N_v \exp\left(\frac{\Phi_{b_L} - E_G + E_{f_p}}{kT}\right) dE_{f_p} = \left[q\mu_p N_v \exp\left(\frac{\Phi_{b_L} - E_G + E_{f_p}}{kT}\right) kT\right]_i^{i+1} \qquad \text{(B-7)}$$

evaluated from i to i+1

$$q\mu_p N_v kT \exp\left(\frac{\Phi_{b_L} - E_{G_i}}{kT}\right)\left[\exp\left(\frac{E_{f_{pi+1}}}{kT}\right) - \exp\left(\frac{E_{f_{pi}}}{kT}\right)\right] \qquad \text{(B-8)}$$

Equating Equations B-6 and 7 yields

$$J_{p,i+\frac{1}{2}} = \frac{\left[\frac{qkT\mu_p N_v \exp\left(\frac{-\phi_{bL} - E_G}{kT}\right)}{H}\right]\left[\exp\left(\frac{E_{fp_{i+1}}}{kT}\right) - \exp\left(\frac{E_{fp_i}}{kT}\right)\right]\left[\frac{\Psi_{i+1}}{kT} - \frac{\Psi_i}{kT}\right]}{\left[\exp\left(\frac{-\Psi_{i+1}}{kT}\right) - \exp\left(\frac{-\Psi_i}{kT}\right)\right]} \quad \text{(B-9)}$$

Using the same approach as above, the corresponding expression for the electron current density is

$$J_{n,i+\frac{1}{2}} = \frac{\left[\frac{qkT\mu_n N_c \exp\left(\frac{-\phi_{bL}}{kT}\right)}{H}\right]\left[\exp\left(\frac{E_{fn_{i+1}}}{kT}\right) - \exp\left(\frac{E_{fn_i}}{kT}\right)\right]\left[\frac{\Psi_{i+1}}{kT} - \frac{\Psi_i}{kT}\right]}{\left[\exp\left(\frac{\Psi_{i+1}}{kT}\right) - \exp\left(\frac{\Psi_i}{kT}\right)\right]} \quad \text{(B-10)}$$

By replacing i+1 with i-1, Δx_{FOR} with Δx_{REV} , and placing a negative sign in front of Equations B-9 and 10, similar expressions can be written for $J_{n,i-1/2}$ and $J_{p,i-1/2}$. Having these four expressions for J_p and J_n for some general points $i+1/2$ and $i-1/2$ allows us now to turn to the original problem of evaluating J_p and J_n in a way that will be numerically stable. This is then done by noting that dJ_p/dx evaluated at i and dJ_n/dx evaluated at i can be written as

$$\left[\frac{dJ_p}{dx}\right]_i = \frac{J_{p_{i+1/2}} - J_{p_{i-1/2}}}{H+h} \quad \text{(B-11)}$$

and

$$\left[\frac{dJ_n}{dx}\right]_i = \frac{J_{n_{i+1/2}} - J_{n_{i-1/2}}}{H+h} \quad \text{(B-12)}$$

APPENDIX C
INSTALLATION

C. 1 System requirement

- 486 with math co-processor (Pentium or better is recommended)
- 16MB RAM (32MB or more is recommended)
- Hard Disk(HD) space required
    - Compact installation 5.3MB
    - Full Installation 10.4MB
    - Run a case 50MB**
- VGA or higher resolution monitor(Super VGA recommended)
- Windows '95 or Windows NT 4.0 (AMPS-1D has not been tested under Windows NT 3.51. If any ones is using Window NT 3.51 and find that it does work, we would appreciated you letting us know.)

** This 50MB on the hard drive is only needed when a case is running.

AMPS-1D will return this disk space after the case is done.

C. 2 Installation Instructions

If you receive 5 disks of AMPS-1D software:

- Locate 'setup.exe' in disk 1 and double click it. AMPS-1D installation/setup will walk you through the installation process.

If you receive AMPS-1D through e-mail or just 1 big file, then follow these instructions:

- Create a temp folder and place AMPS1D.exe in it (note not the short cut of "AMPS1D.EXE",).
- Double click "AMPS1D. EXE ", then close(use [ALT]+[F4]) the self-extracting window when it is done(when "_isdel.exe" appear on the screen.)
- Then locate “Setup.exe” in the above temp folder that you have created and double click "Setup.exe" (this should start the AMPS-1D installation/setup)
- Follow all instructions in AMPS-1D installation/setup
- When it prompts “Finish” then you are set to play with AMPS-1D

NOTE: There is a pre-compiled example in where you have installed AMPS-1D. It is in Samples folder.

C. 3 Running AMPS-1D

To start AMPS-1D, click on the Start button at the lower-left-hand corner of the Windows desktop. Select Programs from the Start menu, and then select “AMPS 1D” from the list of

programs in the cascading window. Click on the AMPS 1D application, and AMPS-1D will be launched.

You can also launch AMPS-1D by double-clicking on any AMPS-1D case file. It has ".AMP" extension. This will automatically launch AMPS-1D and load the selected case.

C. 4 Problems and questions

If you have any problem or question, please send via e-mail to

AMPS@emprl.psu.edu.

You are welcome to visit our web site at

http://www.emprl.psu.edu/amps

for latest news and information.